

4d $\mathcal{N} = 1$ from 6d D-type $\mathcal{N} = (1, 0)$

Jin Chen^a, Babak Haghighat^b, Shuwei Liu^c, and Marcus Sperling^b

^a*CAS Key Laboratory of Theoretical Physics, Institute of Theoretical Physics
Chinese Academy of Sciences, Beijing 100190, China
Email: jinchen@itp.ac.cn*

^b*Yau Mathematical Sciences Center, Tsinghua University
Haidian District, Beijing, 100084, China
Email: babakhaghighat@tsinghua.edu.cn,
marcus.sperling@univie.ac.at*

^c*Department of Physics, Tsinghua University
Haidian District, Beijing, 100084, China
Email: liu-sw15@mails.tsinghua.edu.cn*

Abstract

Compactifications of 6d $\mathcal{N} = (1, 0)$ SCFTs give rise to new 4d $\mathcal{N} = 1$ SCFTs and shed light on interesting dualities between such theories. In this paper we continue exploring this line of research by extending the class of compactified 6d theories to the D -type case. The simplest such 6d theory arises from D5 branes probing D -type singularities. Equivalently, this theory can be obtained from an F-theory compactification using -2 -curves intersecting according to a D -type quiver. Our approach is two-fold. We start by compactifying the 6d SCFT on a Riemann surface and compute the central charges of the resulting 4d theory by integrating the 6d anomaly polynomial over the Riemann surface. As a second step, in order to find candidate 4d UV Lagrangians, there is an intermediate 5d theory that serves to construct 4d domain walls. These can be used as building blocks to obtain torus compactifications. In contrast to the A -type case, the vanishing of anomalies in the 4d theory turns out to be very restrictive and constraints the choices of gauge nodes and matter content severely. As a consequence, in this paper one has to resort to non-maximal boundary conditions for the 4d domain walls. However, the comparison to the 6d theory compactified on the Riemann surface becomes less tractable.

Contents

1	Introduction	1
2	Six dimensions	3
2.1	6d theory	3
2.2	6d anomaly polynomial	3
2.3	Anomaly polynomial after compactification	5
2.4	a -maximisation	7
3	Five dimensions	8
3.1	$\frac{1}{2}$ BPS boundary conditions	8
3.2	Flux domain walls	10
3.3	$\text{Tr}(SU(N \pm 1)^3)$ cubic gauge anomalies	11
3.4	$\text{Tr}(U(1)_R G^2)$ anomalies	14
3.5	Non-maximal boundary conditions	16
4	Four dimensions	19
4.1	Domain wall for non-maximal boundary conditions	19
4.2	Quiver theory on torus	22
4.3	Quiver theory on 2-punctured sphere	27
4.3.1	6d theory on 2-punctured sphere	27
4.3.2	Quiver theory from domain walls	28
5	Conclusions	30
A	Notations, anomalies and β-functions	30

1 Introduction

Recently, a series of interesting works [1–7] initiated a systematic study on compactifications of various 6d $\mathcal{N} = (1, 0)$ SCFTs on Riemann surfaces to obtain a vast class of new 4d $\mathcal{N} = 1$ SCFTs. The corresponding SCFTs in six and four dimensions are then connected through RG flows which preserve certain properties of the 6d fixed point theory along the flow. This construction has given rise to new dualities between 4d $\mathcal{N} = 1$ theories by tracing different theories back to the same 6d origin [7] as well as new asymptotically free UV descriptions of 4d SCFTs.

In all these examples, one starts with a 6d theory obtained by compactifying F-theory on a local elliptic Calabi-Yau threefold. In this construction, as initiated by [8], the geometry of the base B of the Calabi-Yau manifold gives rise to the tensor multiplet sector of the 6d SCFT such that the number of tensor multiplets is equal to the dimension of $H^{1,1}(B, \mathbb{Z})$. Furthermore, the intersection form on B gives the couplings of these tensor multiplets to each other. This intersection form is constrained by the fact that all curve classes inside the base must be simultaneously shrinkable to zero volume in order to restore conformal symmetry at the origin of the tensor branch. As a consequence all curve classes are forced to be \mathbb{P}^1 's which have negative self-intersection number. The elliptic fiber above these curves degenerates and gives rise to gauge groups determined by Kodaira's classification of elliptic fibers in the effective 6d theory. Following the classification of [8],

the \mathbb{P}^1 's in the base can intersect according to a generalised A -type or a generalised D -type quiver, and in cases where all \mathbb{P}^1 's have self-intersection number -2 one can also construct E -type quivers.

Compactifications of such theories to 4d $\mathcal{N} = 1$ was initiated in [1, 2]. Therein, the authors focused on the simplest possibility, namely starting with a 6d theory which arises from an A -type quiver of -2 curves. Already, this simple case gives rise to an immensely rich class of 4d theories admitting asymptotically free UV Lagrangian descriptions. To obtain the theory on a general Riemann surface, one constructs the results for the torus and the three-punctured sphere and all other cases can be obtained by gluing these building blocks. A stepping stone for these constructions is the theory corresponding to the tube, namely the two-punctured sphere. Here, the idea is to first find the circle compactification of the 6d theory giving rise to a 5d gauge theory and subsequently constructing 4d domain walls for these 5d theories by choosing $\frac{1}{2}$ -BPS boundary conditions. In practice, this construction leads to $SU(N)$ (N here being the number of nodes/ \mathbb{P}^1 's in the 6d quiver) gauge nodes forming a tessellation of the tube corresponding to the two-punctured sphere. It is found that the number of the Cartans of the global symmetry group is preserved along the RG flow from 6d to 4d and manifests itself as $U(1)$ flavour symmetries of the 4d Lagrangian theory. Moreover, the 4d theory has further flavour symmetries which correspond to so called *maximal punctures* arising from the 5d boundary conditions at the two ends of the tube. A consistency check for the resulting compactifications is the match of 't Hooft anomalies of the 6d theory on the Riemann surface and the 4d theory. Since the numbers of $U(1)$ flavour symmetries are equal, the central charges of the two theories obtained from a -maximisation are then bound to match.

The story developed in [1, 2], was later generalised to other 6d SCFTs in [3–7]. In [6] it was realised that when compactifying the 6d theory, knowledge of the resulting 5d theory is essential for constructing domain walls and, subsequently, torus compactifications. This recipe works quite well for all of the so-called ADE conformal matter theories [9] as well as for the E-string theory [4] and other minimal 6d SCFTs [7]. One common feature of all such compactifications studied so far is that the 6d theory one starts with is always of generalised A -type. This means that only pairwise intersections between adjacent nodes of the 6d tensor branch are possible and trivalent vertices do not appear.

The goal of the current paper is to extend the above results to the case where the 6d $\mathcal{N} = (1, 0)$ theory is of generalised D -type. The simplest possibility is the case where the discriminant locus of the elliptic fibration of the F-theory compactification is a collection of -2 -curves intersecting according to a D -type quiver. Compactifying such a theory to five dimensions yields a circular quiver with alternating SO and USp nodes [10]. Starting from there, we proceed to construct 4d $\mathcal{N} = 1$ domain wall solutions of the resulting 5d theory and successively glue them together to obtain a torus compactification from 6d. In the case of SO and USp nodes, this process turns out to be subtle as the $\frac{1}{2}$ -BPS conditions of the domain wall cannot retain the full gauge symmetry, but ultimately lead to unitary subgroups of either SO or USp type gauge nodes. When gluing domain walls together by gauging flavour symmetries, one notices that although all cubic gauge anomalies cancel, there are still non-vanishing R-symmetry anomalies of type $R-G-G$. To further cancel such anomalies, we are forced to modify the domain wall construction of this paper by considering non-maximal punctures. It is then apparent that the 4d theories obtained by gluing such domain walls to obtain a candidate torus compactification preserve a lower number of flavour symmetries than the corresponding 6d parent theory. Moreover, carefully performing a -maximisation indicates that these candidate theories flow to free IR theories. As a consequence, potentially existing non-unitary operators in the theory obtained from the 6d compactification present an open problem.

The organisation of the paper is as follows. In Section 2, after a review of the D -type 6d theory and its brane realisation, its anomaly polynomial is computed. Thereafter, a twisted compactification of the theory to four dimensions is performed and a subsequent integration of the anomaly 8-form on the torus yields the anomaly 6-form of the corresponding 4d $\mathcal{N} = 1$ SCFT. By turning

on fluxes for flavour symmetries, the $SU(2k)$ flavour symmetry is broken to its Cartan subgroup $U(1)^{2k-1}$ which mixes with the $U(1)_R$ -symmetry to give rise to a new R-symmetry in the IR. The resulting central charges are computed from a -maximisation. In addition, some comments on compactifications on a 2-sphere with punctures are given. In Section 3 the 4d domain wall theories are constructed by compactifying the 6d theory first to five dimensions and introducing $\frac{1}{2}$ -BPS boundary conditions. Then the 't Hooft anomaly coefficients are computed and it is shown how to choose boundary conditions which lead to the cancellation of all gauge and $U(1)_R$ anomalies. Then in Section 4 all the ingredients are put together to compute the final 4d quiver theory corresponding to torus compactification from 6d. Lastly, Section 5 provides a conclusion as well as an outline of open problems and possible future directions. For convenience, Appendix A provides a summary of conventions relevant for anomaly calculations.

2 Six dimensions

This section reviews the construction of the 6d model of D -type. Thereafter, the anomaly 8-form is derived and subsequently reduced along a Riemann surface. This allows the computation of 4d central charges via a -maximisation.

2.1 6d theory

The 6d $\mathcal{N} = (1, 0)$ of interest admits two constructions. Starting in Type IIB, one can consider the world-volume theory that lives on k D5-branes transverse to a D_{N+1} singularity. As known from the ADE quiver gauge theories [11, 12], the 6d low-energy world-volume can be conveniently summarised in a D_{N+1} -Dynkin type quiver gauge theory. Alternatively, one may employ a Type IIA brane construction of N NS5 branes and $2k$ D6-branes in the presence of an ON^0 -plane. As shown in [13], the ON^0 -plane results in a D -type quiver gauge theory on the tensor branch of the corresponding 6d $\mathcal{N} = (1, 0)$ theory.

Therefore, the 6d $\mathcal{N} = (1, 0)$ theory on the tensor branch includes vector and hypermultiplets which are coupled according to the quiver diagram

$$\begin{array}{c}
 \textcircled{SU(k)} \\
 | \\
 \textcircled{SU(k)} - \textcircled{SU(2k)} - \textcircled{SU(2k)} - \dots - \textcircled{SU(2k)} - \square \textcircled{SU(2k)} \cdot \\
 \underbrace{\hspace{10em}}_{N-1}
 \end{array} \tag{2.1}$$

In addition, there exist $(N + 1)$ tensor multiplets, one for each gauge group factor.

2.2 6d anomaly polynomial

Based on the quiver (2.1), one can derive the anomaly polynomial via using the results of [14, 15]. To arrive at the anomaly 8-form there are several steps to take. To begin with, the 6d $\mathcal{N} = (1, 0)$ multiplets contribute as follows:

- A hypermultiplet transforming in representation ρ :

$$I_8^{\text{hyper}} = \frac{1}{24} \text{Tr}_\rho F^4 + \frac{1}{48} \text{Tr}_\rho F^2 p_1(T) + \frac{d_\rho}{5760} (7p_1^2(T) - 4p_2(T)) , \tag{2.2}$$

where d_ρ denotes the dimension of the representation ρ .

- A vector multiplet of gauge group G :

$$I_8^{\text{vector}} = -\frac{1}{24} \left(\text{Tr}_{\text{adj}} F^4 + 6c_2(R) \text{Tr}_{\text{adj}} F^2 + d_G c_2(R)^2 \right) - \frac{1}{48} \left(\text{Tr}_{\text{adj}} F^2 + d_G c_2(R) \right) p_1(T) - \frac{d_G}{5760} \left(7p_1^2(T) - 4p_2(T) \right) \quad (2.3)$$

and d_G is the dimension of G .

- A tensor multiplet:

$$I_8^{\text{tensor}} = \frac{1}{24} c_2^2(R) + \frac{1}{48} c_2(R) p_1(T) + \frac{1}{5760} \left(23p_1^2(T) - 116p_2(T) \right). \quad (2.4)$$

The notation for the appearing characteristic classes is as follows: $c_2(R)$ for the second Chern classes in the fundamental representations of the 6d $\mathcal{N} = (1, 0)$ $SU(2)_R$ R-symmetries; $p_1(T)$ and $p_2(T)$ for the first and second Pontryagin classes of the tangent bundle. Moreover, F_G denotes the field strength of the flavour symmetry $G = SU(2k)$; and the subscripts ρ, f, adj of a trace indicates with respect to which representation ρ , adjoint, or fundamental the trace is performed.

Then one can determine the anomaly 8-form contributions from the vector and hypermultiplets encoded in the quiver (2.1) as well as the contributions of the $(N+1)$ tensor multiplets. Summing all perturbative contributions of the $\mathcal{N} = (1, 0)$ multiplets, one finds the following pure gauge, mixed gauge R-symmetry, and mixed gauge flavour anomaly terms

$$I_8^{\text{pert}} \supset -\frac{1}{8} (A_{D_{N+1}})^{ij} \text{Tr}_f F_i^2 \text{Tr}_f F_j^2 - \frac{1}{2} \rho^i \text{Tr}_f F_i^2 c_2(R) - 2\gamma^i \text{Tr}_f F_i^2 \text{Tr}_f F_G^2, \quad (2.5)$$

where $i, j = 1, \dots, N+1$ labels the gauge group factors in (2.1). The numbering of the nodes in the underlying D_{N+1} Dynkin diagram follows the conventions of [16, Table IV], i.e. the spinor nodes are labelled by N and $N+1$, respectively; while the node attached to the flavour is labelled by $i = 1$. Moreover, $A_{D_{N+1}}$ denotes the Cartan matrix of D_{N+1} , see [16, Table VI], and the two $(N+1)$ -dimensional vectors ρ, γ are defined as follows:

$$\rho = (2k, 2k, \dots, 2k, k, k), \quad \gamma = -\frac{1}{4}(1, 0, \dots, 0). \quad (2.6)$$

In order to cancel all pure and mixed gauge anomalies, one adds a Green-Schwarz term [17–19]

$$I_8^{\text{GS}} = \frac{1}{2} \Omega^{ij} I_i I_j, \quad (2.7)$$

and the form of the anomalies (2.5) determines the Green-Schwarz term almost uniquely to be

$$\Omega^{ij} = (A_{D_{N+1}})^{ij}, \quad I_i = \frac{1}{2} \text{Tr}_f F_i^2 + (A_{D_{N+1}}^{-1})_{ij} \left(\rho^j c_2(R) + 2\gamma^j \text{Tr}_f F_G^2 \right). \quad (2.8)$$

For the inverse $(A_{D_{N+1}}^{-1})_{ij}$ of the Cartan matrix the reader is referred to [16, Table IV]. Finally, adding the perturbative contribution from the supermultiplets and the GS-term, one arrives at the full anomaly polynomial¹

$$I_8 = \frac{(8N^3 - 4N + 1)k^2 + (N + 1)}{12} c_2(R)^2 - \frac{(2N - 1)k^2 - (N + 1)}{24} c_2(R) p_1(T) - \frac{k(2N - 1)}{2} \text{Tr}_f F_G^2 c_2(R) + \frac{k}{24} \text{Tr}_f F_G^2 p_1(T) + \frac{1}{8} \left(\text{Tr}_f F_G^2 \right)^2 + \frac{k}{12} \text{Tr}_f F_G^4 + \frac{14k^2 + 30(N + 1)}{5760} p_1(T)^2 - \frac{8(k^2 + 15(N + 1))}{5760} p_2(T). \quad (2.9)$$

¹In view of (2.1), the derived anomaly polynomial is valid for $k \geq 2$. The special case $k = 1$ should be considered separately.

For later convenience, consider the flavour and R-symmetry bundles in more detail, see for instance [3]. Suppose the $G = SU(2k)$ flavour symmetry bundle splits, and the Chern roots are given by b_i , $i = 1, \dots, 2k$ satisfying $\sum_{i=1}^{2k} b_i = 0$. Then one finds

$$\mathrm{Tr}_f F_G^2 = -\sum_{i=1}^{2k} b_i^2, \quad \mathrm{Tr}_f F_G^4 = \sum_{i=1}^{2k} b_i^4. \quad (2.10)$$

Similarly, the $SU(2)_R$ bundle splits and has Chern roots $(x, -x)$ such that

$$c_2(R) = -x^2. \quad (2.11)$$

2.3 Anomaly polynomial after compactification

Next, one can compute the anomaly 6-form of a 4d $\mathcal{N} = 1$ theory that originates from the compactification of the 6d $\mathcal{N} = (1, 0)$ theory (2.1) on a Riemann surface with fluxes via the anomaly 8-form (2.9).

Generically, there are two effects to be taken into account when compactifying on a genus g Riemann surface C_g with fluxes. Firstly, to preserve $\mathcal{N} = 1$ supersymmetry in 4d one must perform a twist. Roughly, the 6d Lorentz group decomposes into the 4d Lorentz group times an $SO(2)$ acting on C_g . Breaking the 6d $SU(2)_R$ symmetry to a maximal torus $U(1)_R$, which is the natural candidate for the 4d R-symmetry, one then twists it with the $SO(2)$ to ensure $\mathcal{N} = 1$ supersymmetry in 4d. Consequently, the Pontryagin classes decompose as [2]

$$p_1(T) = t^2 + p_1(T'), \quad p_2(T) = t^2 p_1(T') + p_2(T') \quad (2.12)$$

into 4d Pontryagin classes of the tangent bundle, $p_1(T')$ and $p_2(T')$, and the first Chern class of the Riemann surface, t . For the R-symmetry, the twisted compactification leads to a mixing between the spin connection t on C_g and $c_1(R')$, the first Chern class of the $U(1)_R$ bundle, such that the Chern root becomes

$$x = c_1(R') - \frac{1}{2}t. \quad (2.13)$$

Secondly, the flavour symmetry fluxes break the $SU(2k)$ symmetry to its torus too, i.e.

$$G = SU(2k) \longrightarrow U(1)^{2k-1}. \quad (2.14)$$

Denote by z_i , $i = 1, \dots, 2k$ the fluxes for the Cartan generators of $\mathfrak{u}(1)_{b_i}$ of the 6d flavour symmetry and suppose $c_1(\beta_i)$ are the first Chern classes of line bundles in 4d. Again, the first Chern class of C_g mixes with flavour symmetries and the Chern roots are related via [3]

$$b_i = N c_1(\beta_i) - z_i \frac{t}{2g-2}. \quad (2.15)$$

The constraint $\sum_{i=1}^{2k} b_i = 0$ then implies

$$\sum_{i=1}^{2k} c_1(\beta_i) = 0, \quad \sum_{i=1}^{2k} z_i = 0. \quad (2.16)$$

Note that the Gauss-Bonnet theorem $\int_{C_g} t = 2 - 2g$ leads to

$$\int_{C_g} b_i = z_i, \quad (2.17)$$

which is a measure for the flux on the torus.

Now, to compute the resulting 4d anomaly 6-form one starts from the anomaly 8-form (2.9), inserts the splitting of flavour bundles (2.10) and R-symmetry bundles (2.11), translates the 6d objects via (2.13), (2.15) into 4d quantities, and lastly integrates over the Riemann surface C_g . After careful evaluation, one finds

$$\begin{aligned}
I_6 = & \frac{(g-1)}{3} (k^2 (8N^3 - 4N + 1) + N + 1) c_1(R')^3 \\
& - kN(2N-1) \sum_{i=1}^{2k} z_i c_1(\beta_i) c_1(R')^2 - (g-1)k(2N-1)N^2 \sum_{i=1}^{2k} c_1(\beta_i)^2 c_1(R') \\
& + \frac{(g-1)}{12} (k^2(2N-1) - (N+1)) c_1(R') p_1(T') - \frac{kN}{12} \sum_{i=1}^{2k} z_i c_1(\beta_i) p_1(T') \\
& + \frac{N^3}{12} \left(3 \sum_{i,j=1}^{2k} (z_i c_1(\beta_i) c_1(\beta_j)^2 + z_j c_1(\beta_i)^2 c_1(\beta_j)) + 4k \sum_{i=1}^{2k} z_i c_1(\beta_i)^3 \right)
\end{aligned} \tag{2.18}$$

which still needs to be supplemented by the constraints (2.16).

Example: 2-torus. Specialising the result to the torus T^2 requires a comment as $g = 1$: the singular-looking flux contribution $\frac{t}{2g-2}$ is then understood as 2-form such that the integral over the Riemann surface is -1 , cf. [3, Footnote 2]. With this in mind, the anomaly 6-form reads as

$$\begin{aligned}
I_6|_{T^2} = & -kN(2N-1) \sum_{i=1}^{2k} z_i c_1(\beta_i) c_1(R')^2 - \frac{kN}{12} \sum_{i=1}^{2k} z_i c_1(\beta_i) p_1(T') \\
& + \frac{N^3}{12} \left(3 \sum_{i,j=1}^{2k} (z_i c_1(\beta_i) c_1(\beta_j)^2 + z_j c_1(\beta_i)^2 c_1(\beta_j)) + 4k \sum_{i=1}^{2k} z_i c_1(\beta_i)^3 \right).
\end{aligned} \tag{2.19}$$

As a remark, the anomaly 6-form (2.19) clearly shows that the 4d gravity anomalies $\text{Tr}(U(1)_R)$, $\text{Tr}(U(1)_R^3)$ vanish in the UV.

Example: 2-sphere with s punctures. Considering a 2-sphere with s punctures can be achieved by replacing $g \rightarrow g + \frac{1}{2}s$, then imposing $g = 0$ yields

$$\begin{aligned}
I_6|_{S_s^2} = & \frac{(s-2)}{6} (k^2 (8N^3 - 4N + 1) + N + 1) c_1(R')^3 \\
& - kN(2N-1) \sum_{i=1}^{2k} z_i c_1(\beta_i) c_1(R')^2 - \frac{(s-2)k(2N-1)N^2}{2} \sum_{i=1}^{2k} c_1(\beta_i)^2 c_1(R') \\
& + \frac{(s-2)}{24} (k^2(2N-1) - (N+1)) c_1(R') p_1(T') - \frac{kN}{12} \sum_{i=1}^{2k} z_i c_1(\beta_i) p_1(T') \\
& + \frac{N^3}{12} \left(3 \sum_{i,j=1}^{2k} (z_i c_1(\beta_i) c_1(\beta_j)^2 + z_j c_1(\beta_i)^2 c_1(\beta_j)) + 4k \sum_{i=1}^{2k} z_i c_1(\beta_i)^3 \right).
\end{aligned} \tag{2.20}$$

In addition, one has to take the contributions from the punctures into account too, which are essentially constant shifts to the IR a -central charge, see for instance [7]. This additional contribution is discussed in Section 3.5 and becomes relevant in Section 4.3.

2.4 a -maximisation

Next, consider the a -maximisation [20] of the 4d $\mathcal{N} = 1$ theory with anomaly polynomial (2.18), assuming that the constraints (2.16) are imposed. The trial R -charge is a linear combination of the UV $U(1)_R$ R -charge and the different $U(1)_{b_i}$ from the maximal torus of the 6d flavour symmetry, i.e.

$$U(1)_R^{\text{trial}} = U(1)_R + \sum_{i=1}^{2k-1} x_i U(1)_{b_i} \quad \text{s.t.} \quad R_{\text{trial}} = R_{UV} + \sum_{i=1}^{2k-1} x_i \beta_i, \quad x_i \in \mathbb{R}. \quad (2.21)$$

Then the trial a -central charge becomes

$$\begin{aligned} a_{\text{trial}} &= \frac{3}{32} (3\text{Tr}R_{\text{trial}}^3 - \text{Tr}R_{\text{trial}}) \\ &= \frac{3}{32} \left(3\text{Tr}(R_{UV}^3) + 9 \sum_i x_i \text{Tr}(R_{UV}^2 \beta_i) + 9 \sum_{i,j} x_i x_j \text{Tr}(R_{UV} \beta_i \beta_j) \right. \\ &\quad \left. + 3 \sum_{i,j,k} x_i x_j x_k \text{Tr}(\beta_i \beta_j \beta_k) - \text{Tr}(R_{UV}) - \sum_i x_i \text{Tr}(\beta_i) \right). \end{aligned} \quad (2.22)$$

The trace coefficients can be read off from (2.19); see examples below. Next, the a -maximisation procedure requires to solve

$$\frac{\partial a_{\text{trial}}}{\partial x_i} = 0, \quad \forall i = 1, \dots, 2k-1. \quad (2.23)$$

However, due to the large number of equations as well as the equally large number of free fluxes z_i , the analytic evaluation is cumbersome. To gain some understanding, one may resort to examples with low value of k and equal fluxes $z_i = z$ for all $i = 1, \dots, 2k-1$.

For the 2-torus, one finds the following contributions to the trial central charge:

$$\text{Tr}(R_{UV}) = -24 \cdot [I_6|_{T^2}]_{c_1(R')p_1(T')} = 0, \quad (2.24a)$$

$$\text{Tr}(R_{UV}^3) = 6 \cdot [I_6|_{T^2}]_{c_1(R')^3} = 0, \quad (2.24b)$$

$$\text{Tr}(\beta_i) = -24 \cdot [I_6|_{T^2}]_{c_1(\beta_i)p_1(T')} , \quad (2.24c)$$

$$\text{Tr}(\beta_i \beta_j \beta_k) = d_{ijk} \cdot [I_6|_{T^2}]_{c_1(\beta_i)c_1(\beta_j)c_1(\beta_k)} , \quad (2.24d)$$

$$\text{Tr}(R_{UV}^2 \beta_i) = 2 \cdot [I_6|_{T^2}]_{c_1(R')^2 c_1(\beta_i)} , \quad (2.24e)$$

$$\text{Tr}(R_{UV} \beta_i \beta_j) = d_{ij} \cdot [I_6|_{T^2}]_{c_1(R')c_1(\beta_i)c_1(\beta_j)} , \quad (2.24f)$$

where $[I_6|_{T^2}]_X$ denotes the coefficient of the combination of characteristic classes X in the anomaly 6-form (2.19). Moreover, $d_{i_1 i_2 \dots i_n}$ equals $m!$ with m being the number of equal indices in $i_1 i_2 \dots i_n$.

Example $k = 2$. For $k = 2$ and equal fluxes, the analytic solution to (2.23) is found to be

$$x_i = -\frac{\sqrt{9N-4}}{6\sqrt{2}N}, \quad i = 1, 2, 3 \quad \Rightarrow \quad a = \frac{z}{\sqrt{2}} (9N-4)^{\frac{3}{2}}. \quad (2.25)$$

Example $k = 3$. For $k = 3$ and equal fluxes, the analytic solution to (2.23) is found to be

$$x_i = -\frac{\sqrt{9N-4}}{9\sqrt{2}N}, \quad i = 1, \dots, 5 \quad \Rightarrow \quad a = \frac{5z}{2\sqrt{2}} (9N-4)^{\frac{3}{2}}. \quad (2.26)$$

Example $k = 4$. For $k = 4$ and equal fluxes, the analytic solution to (2.23) is found to be

$$x_i = -\frac{\sqrt{9N-4}}{12\sqrt{2N}}, \quad i = 1, \dots, 7 \quad \Rightarrow \quad a = \frac{7\sqrt{2}z}{3} (9N-4)^{\frac{3}{2}}. \quad (2.27)$$

3 Five dimensions

The 6d theory (2.1) can be compactified on S^1 . The resulting 5d theory has a low-energy description in terms of a 5d $\mathcal{N} = 1$ affine A_{2k-1} quiver gauge theory with alternating $SO(2k+2)$ and $USp(2k-2)$ gauge nodes [10], i.e.

$$\begin{array}{ccccccc}
 USp(2N-2) & SO(2N+2) & \cdots & USp(2N-2) & SO(2N+2) & & \\
 \circ & \circ & \cdots & \circ & \circ & & \\
 | & | & & | & | & & \\
 \circ & \circ & \cdots & \circ & \circ & & \\
 SO(2N+2) & USp(2N-2) & \cdots & SO(2N+2) & USp(2N-2) & &
 \end{array}
 \left. \begin{array}{l} \\ \\ \\ \end{array} \right\} \begin{array}{l} k \times SO(2N+2) \text{ nodes,} \\ k \times USp(2N-2) \text{ nodes} \end{array}. \quad (3.1)$$

This 5d theory will be the basis for the construction of flux domain wall theories in the spirit of [21], see also [4, 5, 22].

3.1 $\frac{1}{2}$ BPS boundary conditions

Similar to the approach taken in [6], one considers the boundary conditions for vector and hypermultiplets that need to be imposed in order to define a domain wall.

Preserve symplectic gauge group. To begin with, focus on the $USp(2N-2)$ gauge nodes and impose Neumann boundary conditions on the gauge field, i.e.

$$A_4^{USp(2N-2)}|_{x^4=0} = 0 = \partial_4 A_\mu^{USp(2N-2)}|_{x^4=0}, \quad \text{for } \mu = 0, 1, 2, 3, \quad (3.2)$$

which preserve the full gauge group. On the other hand, Dirichlet boundary conditions are imposed on the adjoint chiral $\Phi^{USp(2N-2)}$ in the 5d $\mathcal{N} = 1$ gauge multiplet, i.e.

$$\Phi^{USp(2N-2)}|_{x^4=0} = 0. \quad (3.3)$$

Next, the hypermultiplets connecting a $USp(2N-2)$ and a $SO(2N+2)$ gauge node transform in the fundamental representation of $USp(2N-2)$ and in the vector representation of $SO(2N+2)$. Hence, viewed from the $USp(2N-2)$ gauge node there are $(N+1)$ copies of fundamental hypers, i.e.

$$H_i = (X_i, Y_i^\dagger), \quad \text{for } i = 1, 2, \dots, N+1. \quad (3.4)$$

Unlike the case of bifundamental hypermultiplets of unitary gauge groups, the two $\mathcal{N} = 1$ chiral multiplets are not in inequivalent representations. To see this, recall that fundamental representation of $USp(2N-2)$ is pseudoreal; hence, the flavour symmetry group for $(N+1)$ copies enhances from $SU(N+1)$ to $SO(2N+2)$. Turning to boundary conditions for H_i , one has the following two options for each $i = 1, 2, \dots, N+1$ that preserve half the supersymmetries:

$$+) \quad \partial_4 X_i|_{x^4=0} = Y_i|_{x^4=0} = 0, \quad \text{or} \quad -) \quad X_i|_{x^4=0} = \partial_4 Y_i|_{x^4=0} = 0. \quad (3.5)$$

Denote the $(N+1)$ -dimensional vector of boundary conditions by σ with components $\sigma_i = \pm$. Naively, one would conclude that there are 2^{N+1} choices for all $N+1$ hypermultiplets. However,

since X_i and Y_i^\dagger transform in equivalent representations of $USp(2N-2)$, any of these choices leads to $(N+1)$ chiral multiplets in the fundamental $USp(2N-2)$ representation. Consequently, the $(N+1)$ chiral multiplets admit at most a $SU(N+1) \subset SO(2N+2)$ flavour symmetry. The important question is, whether the choice σ of boundary conditions implies that the chirals transform in the fundamental or anti-fundamental representation of $SU(N+1)$. Consider the two extreme cases $\sigma_\pm \equiv (\pm, \dots, \pm)$, meaning either all X_i survive for σ_+ or all Y_i survive for σ_- . Then the origin of the enhanced flavour symmetry implies that the X_i furnish the fundamental and the Y_i the anti-fundamental representation of $SU(N+1)$. The choice of a generic boundary condition differs from the extreme case only by a different embedding $SU(N+1) \hookrightarrow SO(2N+2)$. In particular, if σ is a fixed choice, then there exists the "opposite" choice $-\sigma$, where all signs are reverted, such that $-\sigma$ corresponds to the same embedding, but the surviving $(N+1)$ chirals transform in the conjugate $SU(N+1)$ representation compared to the ones from σ . Consequently, it is sufficient to consider the extreme cases σ_\pm .

Turning to the $SO(2N+2)$ gauge nodes, it is suggestive to impose Neumann boundary conditions on the $SU(N+1)$ subgroup resulting from the chiral matter fields and set the remaining gauge field components to zero, i.e.

$$A_4^{SO(2N+2)}|_{x^4=0} = \partial_4 A_\mu^{SO(2N+2)}|_{x^4=0} = A_\mu^{SO(2N+2) \setminus SU(N+1)}|_{x^4=0} = 0 \quad \text{for } \mu = 0, 1, 2, 3. \quad (3.6)$$

Meanwhile, Dirichlet boundary conditions are imposed on the full adjoint chiral of the 5d $\mathcal{N} = 1$ $SO(2N+2)$ gauge multiplet, i.e.

$$\Phi^{SO(2N+2)}|_{x^4=0} = 0. \quad (3.7)$$

Therefore, the boundary conditions defined in (3.2), (3.3), (3.5), (3.6) and (3.7) specify one chamber of the 5d theory on the interface. For each of the $2k$ hypermultiplets in (3.1) one may choose boundary conditions σ_\pm , such that the theory is determined by a $(2k)$ -dimensional vector \mathbb{B} . Here, the convention is that σ_+ turns the hypermultiplets into a chiral in the fundamental representation of $SU(N+1)$, while σ_- corresponds to the anti-fundamental. To exemplify a few cases, one may consider

$$\mathbb{B} = (\dots, +, +, -, -, +, \dots) \quad \dots \begin{array}{c} \xrightarrow{SU(N+1)} \text{---} \text{---} \text{---} \text{---} \xrightarrow{SU(N+1)} \\ \text{---} \text{---} \text{---} \text{---} \xrightarrow{USp(2N-2)} \text{---} \text{---} \text{---} \text{---} \xrightarrow{USp(2N-2)} \end{array} \dots, \quad (3.8a)$$

$$\mathbb{B} = (\dots, -, -, -, +, +, \dots) \quad \dots \begin{array}{c} \xrightarrow{SU(N+1)} \text{---} \text{---} \text{---} \text{---} \xrightarrow{SU(N+1)} \\ \text{---} \text{---} \text{---} \text{---} \xrightarrow{USp(2N-2)} \text{---} \text{---} \text{---} \text{---} \xrightarrow{USp(2N-2)} \end{array} \dots. \quad (3.8b)$$

Preserve orthogonal gauge group. On the other hand, one can equally well impose Neumann boundary conditions on the $SO(2N+2)$ gauge nodes to preserve the entire gauge group, i.e.

$$A_4^{SO(2N+2)}|_{x^4=0} = \partial_4 A_\mu^{SO(2N+2)}|_{x^4=0} = 0, \quad \text{for } \mu = 0, 1, 2, 3, \quad (3.9)$$

and similarly Dirichlet boundary conditions on the adjoint chiral $\Phi^{SO(2N+2)}$ in the 5d $\mathcal{N} = 1$ $SO(2N+2)$ gauge multiplet,

$$\Phi^{SO(2N+2)}|_{x^4=0} = 0. \quad (3.10)$$

Viewed from the $SO(2N+2)$ gauge group, the hypermultiplets

$$H'_a = (X'_a, Y_a'^\dagger) \quad \text{for } a = 1, \dots, N-1 \quad (3.11)$$

between this gauge group and the adjacent gauge node are understood as $(N - 1)$ copies of fundamental $SO(2N+2)$ hypermultiplets. Again, the two $\mathcal{N} = 1$ chirals in each H'_a are in equivalent $SO(2N+2)$ representations, which is the reason for the flavour symmetry enhancement $SU(N-1) \rightarrow USp(2N-2)$. By assigning $\frac{1}{2}$ BPS boundary conditions to the hypermultiplets, one has two choices

$$+') \quad \partial_4 X'_a|_{x^4=0} = Y'_a|_{x^4=0} = 0, \quad \text{or} \quad -') \quad X'_a|_{x^4=0} = \partial_4 Y'_a|_{x^4=0} = 0, \quad (3.12)$$

for each $a = 1, \dots, N - 1$. Nevertheless, all of these choices result in $(N - 1)$ chiral multiplets in the fundamental $SO(2N+2)$ representation. The flavour symmetry of these $(N - 1)$ chirals is at most $SU(N-1) \subset USp(2N-2)$, but one has to determine whether they transform in the fundamental or anti-fundamental representation. Analogous to the above arguments, one could summarise the choices in (3.12) in a $(N - 1)$ -dimensional vector σ' , with components \pm . Again, the extreme cases $\sigma'_\pm \equiv (\pm, \dots, \pm)$ indicate that choosing X'_a only leads to chirals in the fundamental of $SU(N-1)$, while the Y'_a choice yields anti-fundamental chirals. Any other choice of σ' characterises a different embedding $SU(N-1) \hookrightarrow USp(2N-2)$, but effectively reduces to chirals transforming in the fundamental or anti-fundamental of $SU(N-1)$ for either σ' or the opposite choice $-\sigma'$. Thus, the two extreme cases are sufficient. Next, one should impose boundary conditions on the $USp(2N-2)$ gauge multiplet that are compatible with the choice of an $SU(N-1)$ subgroup. In detail,

$$A_4^{USp(2N-2)}|_{x^4=0} = \partial_4 A_\mu^{USp(2N-2)}|_{x^4=0} = A_\mu^{USp(2N-2) \setminus SU(N-1)}|_{x^4=0} = 0 \quad \text{for} \quad \mu = 0, 1, 2, 3, \quad (3.13)$$

and $\Phi^{USp(2N-2)}|_{x^4=0} = 0$.

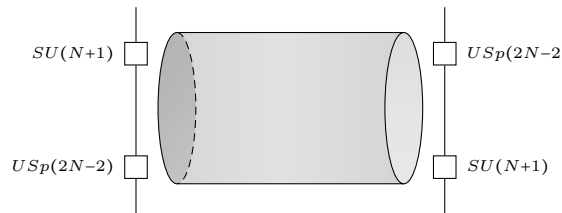
The boundary conditions of (3.9), (3.10), (3.12), and (3.13) determine another type of chamber of the 5d theory on the interface which is specified by an $(2k)$ -dimensional vector \mathbb{B}' . The convention is as above, if σ'_+ then the surviving chiral multiplets are $SU(N-1)$ fundamentals, while anti-fundamentals for σ'_- . The resulting theory can be illustrated in a few examples:

$$\mathbb{B}' = (\dots, +, +, -, -, +, \dots) \quad \dots \rightarrow \underset{SO(2N+2)}{\circ} \xleftarrow{SU(N-1)} \underset{SO(2N+2)}{\circ} \xleftarrow{SU(N-1)} \underset{SO(2N+2)}{\circ} \rightarrow \dots, \quad (3.14a)$$

$$\mathbb{B}' = (\dots, -, -, -, +, +, \dots) \quad \dots \xleftarrow{SU(N-1)} \underset{SO(2N+2)}{\circ} \xleftarrow{SU(N-1)} \underset{SO(2N+2)}{\circ} \xleftarrow{SU(N-1)} \dots. \quad (3.14b)$$

3.2 Flux domain walls

With the preparation from Section 3.1, one can construct a flux domain wall as the interface theories between two 5d chambers. From the perspective of the original 6d theories, the domain wall theories can be regarded as compactifications of the 6d theories on a tube or, say, a sphere with two punctures. These punctures are then associated to the gauge groups of the 5d quiver theory. If one removes the gauge multiplets, they will be treated as the corresponding non-Abelian global symmetries, in addition to the 6d global symmetries $SU(2k)$. More concretely, in the cases introduced in Section 3.1, there exist two types of puncture symmetries: $USp(2N-2)$ - $SU(N+1)$ and $SO(2N+2)$ - $SU(N-1)$. Consequently, three types of fundamental domain walls arise:



$$(3.15a)$$

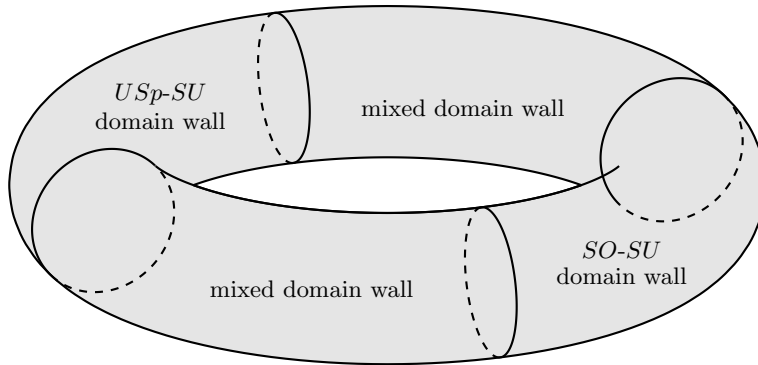


Figure 1: Example of a 4d theory on a torus constructed from a USp - SU domain wall (3.15a) and a SO - SU domain wall (3.15b) such that both are glued to two mixed domain walls (3.15c).

$$\begin{array}{ccc}
 \begin{array}{c}
 \text{---} \\
 \square \\
 \text{---}
 \end{array}
 &
 \begin{array}{c}
 \text{---} \\
 \square \\
 \text{---}
 \end{array}
 &
 \begin{array}{c}
 \text{---} \\
 \square \\
 \text{---}
 \end{array}
 \end{array}
 \quad (3.15b)$$

$$\begin{array}{ccc}
 \begin{array}{c}
 \text{---} \\
 \square \\
 \text{---}
 \end{array}
 &
 \begin{array}{c}
 \text{---} \\
 \square \\
 \text{---}
 \end{array}
 &
 \begin{array}{c}
 \text{---} \\
 \square \\
 \text{---}
 \end{array}
 \end{array}
 \quad (3.15c)$$

In order to obtain the desired 4d theories, the vector multiplets have to be added back, i.e. they gauge the global symmetries associated to the punctures. Therefore, the 4d theories on a torus can be constructed via gluing the fundamental domain walls along their punctures. For example, a torus theory constructed from four domain walls can be sketched as in Figure 1. Nevertheless, all these fundamental domain walls potentially suffer from various anomalies. In particular, one has to guarantee that the glued $SU(N \pm 1)$ gauge nodes are free of the cubic gauge anomalies, i.e.

$$\text{Tr}(SU(N \pm 1)^3) = 0. \quad (3.16)$$

These gauge anomalies are the focus of the next section.

3.3 $\text{Tr}(SU(N \pm 1)^3)$ cubic gauge anomalies

Since all three fundamental domain walls (3.15) contain unitary gauge nodes, they will be discussed separately. Appendix A provides the conventions for the anomaly coefficients. Without loss of generality, one may consider the $k = 1$ case, i.e. the 5d theory (3.1) consists only of one $USp(2N-2)$ and one $SO(2N+2)$ node, to construct the domain walls. This $k = 1$ is only used to simplify the presentation, but any comparison to 6d requires $k \geq 2$.

$USp(2N-2)$ - $SU(N+1)$ domain walls. To begin with, focus on the domain wall (3.15a) and $k = 1$. Consequently, each chamber of the domain wall contains one $USp(2N-2)$ and one $SU(N+1)$

node. To connect the chambers, one includes additional 4d chiral fields q to each node, which are oriented from left to right. Then there are two choices for which nodes between the two chambers the chirals q connect: either the $USp-SU$ and $SU-USp$ nodes, or $USp-USp$ and $SU-SU$ nodes. In addition, for each choice, there exist four types of boundary conditions that can be assigned on the 5d hypermultiplets of the two chambers. Following Section 3.1, these boundary conditions are denoted by $(+, +)$, $(+, -)$, $(-, +)$, and $(-, -)$. If one chooses to connect the $USp-SU$ and $SU-USp$ nodes in the two chambers, then the boundary conditions for the 5d fields of left and right chamber have to be opposite to each other. As a consequence, the boundary conditions of the 5d fields together with the choice of chiral fields q determine how to include additional 4d chiral fields \tilde{q} that serve to formulate cubic superpotentials and triangulate the domain walls. In total there are eight different $USp(2N-2)-SU(N+1)$ domain walls for the $k = 1$ case. To illustrate the construction, the fundamental domain wall with $(+, -)$ boundary conditions on the left and $(-, +)$ on the right is given by

(3.17)

and the need for the additional loops A and \bar{A} can be seen as follows: From 4d perspective, (3.17) is an $\mathcal{N} = 1$ Wess-Zumino model with non-Abelian global symmetries $USp(2N-2)^2 \times SU(N+1)^2$. In order to glue this domain wall with others, one further needs to require that the cubic gauge anomaly of $SU(N+1)$ nodes vanishes. For example, consider the lower left $SU(N+1)$ node to be specific. Then the 4d chiral fields q_2 and \tilde{q}_1 contribute $-(2N-2)$ and $(N+1)$ units to the cubic anomaly, respectively. The two vertical chiral fields, as residues of the 5d hypermultiplets, also contribute to cubic anomaly with an additional factor of $\frac{1}{2}$, as a consequence of 5d anomaly inflow, see [6]. In this quiver, the net cubic anomaly from the two vertical chirals is zero due to our chosen boundary condition. Summing up all the contributions, the cubic anomaly becomes

$$\text{Tr}(SU(N+1)^3) = -(2N-2) + (N+1) = -(N+1-4). \quad (3.18)$$

Therefore, one additional anti-symmetric chiral matter fields A is required to cancel the anomaly of the $SU(N+1)$ node.

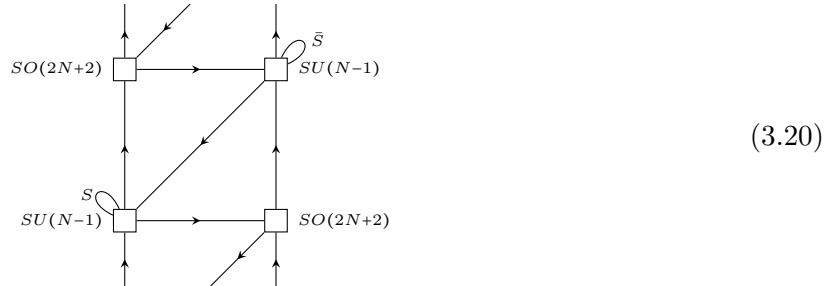
Analogously, one can show that the upper right $SU(N+1)$ node in (3.17) requires another matter fields \bar{A} in the conjugate representation of the anti-symmetric representation to cancel the cubic gauge anomaly. Thus, the domain wall becomes anomaly free if the additional loops A and \bar{A} are added to the construction as shown in (3.17).

From the quiver diagram, it is straightforward to derive the $\mathcal{N} = 1$ superpotential. Besides the cubic superpotential terms that stem from triangles in (3.17), one needs also form superpotentials for the anti-symmetric fields A and \bar{A} via

$$\mathcal{W} = \text{Tr}(Jq_1\bar{A}q_1 + Jq_2Aq_2) + \text{cubic terms}, \quad (3.19)$$

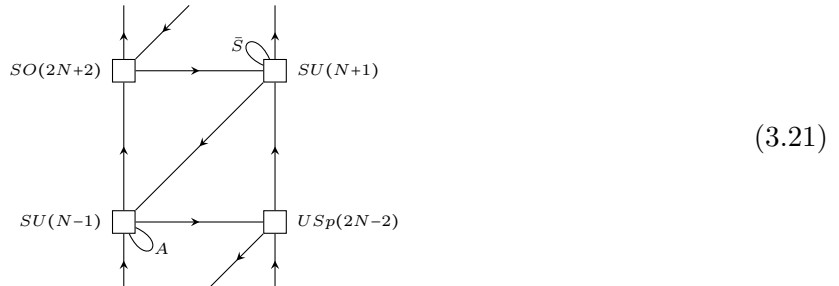
where J is the anti-symmetric tensor of $USp(2N-2)$.

$SO(2N+2)$ - $SU(N-1)$ domain walls. Analogous to the above analysis, there exist eight different SO - SU domain walls (3.15b) in the $k = 1$ case, which follow from the four types of boundary conditions assigned to the 5d fields and the subsequent two choices of how to connect the 5d chambers via additional 4d chiral fields. As an example, consider the domain wall with boundary conditions $(+, -)_{L,R}$ such that the SO - SU and SU - SO nodes are paired up. In order to have vanishing cubic gauge anomalies for the $SU(N-1)$ nodes, one has to add one symmetric matter field for each $SU(N-1)$ node. Collecting all the ingredients, one ends up with the following theory:



It is then straightforward to verify the vanishing cubic anomalies for the two $SU(N-1)$ nodes. Moreover, the superpotential can be derived in similar fashion as in the USp - SU case.

$USp(2N-2)$ - $SO(2N+2)$ - $SU(N\pm 1)$ mixed domain walls. Lastly, consider the mixed domain wall (3.15c) as the interface theory of a $USp(2N-2)$ - $SU(N+1)$ and a $SO(2N+2)$ - $SU(N-1)$ chamber. Unfortunately, it turns out that there is no way to construct a cubic anomaly free mixed domain wall for certain choices of boundary conditions. For instance, consider the mixed domain wall corresponding to $(+, -)_L, (-, +)_R$ boundary conditions, which is given by



One can check that the $SU(N \pm 1)$ nodes, even when supplemented with (anti-)symmetric matter fields, are anomalous, i.e.

$$\text{Tr}(SU(N+1)^3) = (2N+2) - (N-1) - (N+1+4) = -2, \quad (3.22a)$$

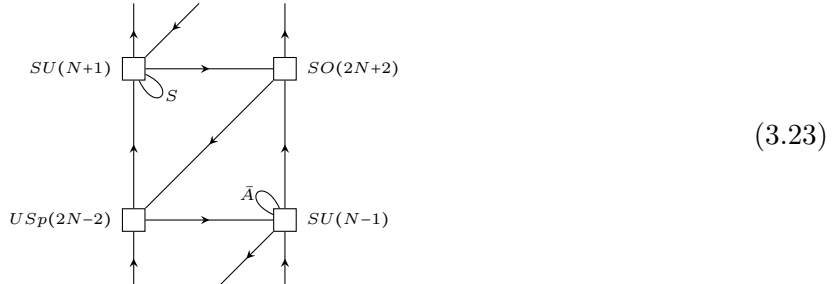
$$\text{Tr}(SU(N-1)^3) = -(2N-2) + (N+1) + (N-1-4) = -2. \quad (3.22b)$$

Of course, the anomalous domain wall cannot be glued to other anomaly free domain walls. Nevertheless, it is possible to find other domain walls with anomalies of opposite and glue these consistently. For example, one may glue the anomalous domain wall (3.21) with another anomalous

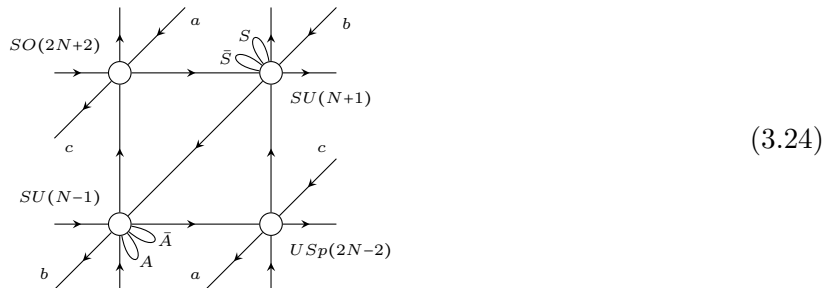
Fields	vertical/diagonal	horizontal	(anti-)symmetric
$U(1)_R$	1	0	2

Table 1: $U(1)_R$ -charge assignments for chiral superfields in the domain walls.

domain wall of the form



which has +2 cubic $SU(N \pm 1)$ anomalies. A calculation proves that the two mixed domain walls (3.21) and (3.23) can be glued to form an anomaly free 4d theory on a torus given by the quiver



However, since all the gauge nodes have positive β -functions one would expect that the theory (3.24) is IR free. Moreover, the $U(1)_R$ -charge anomalies of (3.24) fail to match with the 6d predictions. Therefore, the next section focuses on more constraints in order to screen out possible 4d candidate theories on a torus.

3.4 $\text{Tr}(U(1)_R G^2)$ anomalies

Next consider the $U(1)_R$ -current anomalies. The $U(1)_R$ symmetry is the maximal torus of the $SU(2)_R$ inherited from the 6d/5d origin and, thus, not the genuine R -symmetry of the corresponding 4d SCFT in the IR. In this paper, the assumption is that this $U(1)_R$ symmetry is preserved in the domain walls as well as the 4d quiver theories on torus. One expects that the $U(1)_R$ mixes with other global $U(1)$ flavour symmetries. Therefore, the genuine IR R -symmetry can be determined via a -maximisation.

Since the UV $U(1)_R$ -symmetry is the maximal torus of the $SU(2)_R$, the hypermultiplets in the 5d quiver theory (3.1) can be normalised to have $U(1)_R$ -charge 1. As a consequence, the inherited (vertical) chiral fields of the domain wall theories have unity $U(1)_R$ -charge too. Following [5, 6, 21], one may assign $U(1)_R$ -charge 0 to the horizontal chiral matter fields q . Then, the $U(1)_R$ -charges of all remaining chiral superfields are determined via the superpotential. The $U(1)_R$ -charge assignment for the quiver theories used in this paper are summarised in Table 1. With the $U(1)_R$ -charge

at hand, one can analyse the potential $\text{Tr}(U(1)_R G^2)$ anomalies that may prevent a consistent gluing of various domain walls via gauging the corresponding non-Abelian $G = USp, SO, SU$ groups. Note that one needs to add a $\mathcal{N} = 1$ vector multiplet in order to gauge a non-Abelian gauge group G , and the associated gauginos have $U(1)_R$ -charge 1, due to the 5d origin. The contributions to $\text{Tr}(U(1)_R G^2)$ from the vertical chiral superfields and the gauginos should be treated as 5d anomaly inflow, as before, and, thus, appear with an additional $\frac{1}{2}$ prefactor. From 4d perspective, this $\frac{1}{2}$ factor can be interpreted as avoiding double counting of the common gaugino and chiral multiplet contribution when gluing two domain walls.

Due to the assumption that the glued domain walls and further quiver theories on torus preserve the $U(1)_R$ symmetry, it is natural to impose the constraint

$$\text{Tr}(U(1)_R G^2) = 0, \quad (3.25)$$

for all $G = USp, SO, SU$ groups. However, a computations show that none of the previous cubic-anomaly-free domain wall satisfies the constraint (3.25). For instance, consider the domain wall (3.17), then one computes the anomaly

$$\text{Tr}(U(1)_R USp(2N-2)^2) = (0-1) \cdot (N+1) + \frac{1}{2}(2N-2+2) = -1 \quad (3.26)$$

for both $USp(2N-2)$ nodes in the quiver. The non-zero anomaly signals that this domain wall cannot be glued with another $U(1)_R$ -anomaly-free domain wall. Nonetheless, one may try to weaken the constraint (3.25): If there would exist a domain wall with $\text{Tr}(U(1)_R USp(2N-2)^2) = +1$ anomaly, one could glue these two anomalous domain walls while preserving the $U(1)_R$ symmetry in the resulting theory.

Based on the above analysis, one can exhaust all possible domain walls for a given k with various boundary conditions, compute their cubic gauge and $\text{Tr}(U(1)_R G^2)$ anomalies, and then combine those with both opposite cubic anomalies for SU nodes, and opposite $\text{Tr}(U(1)_R G^2)$ anomalies for all $G = USp, SO, SU$ nodes. However, it turns out that no domain wall pairing can simultaneously satisfy both the cubic and the $\text{Tr}(U(1)_R G^2)$ anomaly conditions. In fact, the vertical and diagonal chiral fields with R -charge 1 do not contribute to $\text{Tr}(U(1)_R G^2)$. Thus, the $\text{Tr}(U(1)_R G^2)$ values for each $G = USp, SO, SU$ node of a given type of domain walls is always independent on the boundary conditions imposed. The implication seems to be that one cannot preserve the $U(1)_R \subset SU(2)_R$ symmetry with R -charge assignments of Table 1 for the domain walls constructed from USp, SO, SU punctures.

One possibility to resolve the matter is to assign different R -charges to all chiral fields. Then, the cubic gauge and $\text{Tr}(U(1)_R G^2)$ anomalies serve as constraints to determine possible R -charge assignments. There are two scenarios to consider: On the one hand, assume that the $U(1)_R \subset SU(2)_R$ is preserved during the domain wall construction. Then the vertical chiral fields, which are induced from 5d hypermultiplets, will inherit the $U(1)_R$ -charge as before, i.e. $U(1)_R$ -charge equal to 1. Assigning different $U(1)_R$ -charges to the horizontal chiral multiplets determines the R -charges of all other chiral fields. However, a computations shows that there does not exist an R -charge assignment that satisfies all three $\text{Tr}(U(1)_R G^2)$ anomaly constraints simultaneously.

On the other hand, one may assume that the $U(1)_R \subset SU(2)_R$ is broken in the domain wall construction. Then the broken $U(1)_R$ symmetry could be mixed with another broken $U(1)$ flavour symmetry to form a new $U(1)'_R$ symmetry. This would allow to assign $U(1)'_R$ -charges different from 1 to the vertical chiral fields. Subsequently, the new freedom allows for a charge assignment compatible with the vanishing of all $\text{Tr}(U(1)'_R G^2)$ anomalies.

Nevertheless, choosing to work with the $U(1)'_R$ symmetry means that one can no longer compare to the 4d results obtained from compactifications of the 6d anomaly polynomial. For example, the

4d anomaly polynomial (2.19) imposes two additional constraints from vanishing $U(1)_R$ -gravity anomalies, $\text{Tr}(U(1)_R) = \text{Tr}(U(1)_R^3) = 0$. Moreover, there are predictions from 6d for various $\text{Tr}(U(1)_R U(1)_{F_i} U(1)_{F_j})$ anomalies, all of which have to be matched with any 4d candidate theory. Therefore, in this paper it is assumed that the $U(1)_R \subset SU(2)_R$ symmetry is unbroken in the domain walls and quiver theories on torus. To circumvent the problem of non-vanishing $\text{Tr} SU^3$ and $\text{Tr}(U(1)_R G^2)$ anomalies, the domain wall theories are changed by considering *non-maximal* boundary conditions on the vector and hypermultiplets of the 5d quiver theory. The domain wall theories obtained via the non-maximal boundary conditions have puncture symmetries that are smaller rank subgroups of $USp(2N-2)$ and $SO(2N+2)$, see also [21].

3.5 Non-maximal boundary conditions

The necessity to introduce domain walls with non-maximal boundary conditions can be traced back to (3.26). If there would be a domain wall with $SU(N)$ - $USp(2N-2)$ punctures, then the $\text{Tr}(U(1)_R G^2)$ vanishes for both $G = SU(N)$ and $USp(2N-2)$. To achieve that one has to assign non-maximal boundary conditions for the hypermultiplets as well as gauge multiplets correspondingly.

Boundary conditions for domain wall. The general idea to assign non-maximal boundary conditions is as follows: For a $USp(2N-2)$ gauge node with $(N+1)$ attached hypermultiplets, for instance, one notices from the 5d quiver (3.1) that these $(N+1)$ hypermultiplets can be treated as $(2N+2)$ half-hypermultiplets, or say chirals, and their global symmetry is gauged by a 5d $\mathcal{N} = 1$ $SO(2N+2)$ gauge multiplet. If one removes this $SO(2N+2)$ gauge multiplet, the half-hypers would at most have a $SU(2N+2)$ flavor symmetry. Now, when two 5d theories are placed at the interface, for example at $x_4 = 0$, to construct a domain wall, one can assign mixed boundary conditions to the $(2N+2)$ half-hypermultiplets. Generalising the discussion of Section 3.1, some number of chiral multiplets are assigned Dirichlet boundary conditions, while the remaining fields obey Neumann boundary conditions such that only a smaller flavour group $H \subset SU(2N+2)$ is preserved. As long as H can be embedded into $SO(2N+2)$, one can add back part of the $SO(2N+2)$ gauge multiplet to gauge this flavour symmetry H . The mixed boundary conditions imposed on the hypermultiplets always preserve half of the 5d $\mathcal{N} = 1$ supersymmetries, just like the $\frac{1}{2}$ BPS conditions do. On the other hand, one assigns Neumann boundary conditions to the gauge fields components in the subgroup H , and Dirichlet boundary conditions to the rest of gauge degrees of freedom. The adjoint chiral multiplet in the 5d $\mathcal{N} = 1$ $SO(2N+2)$ gauge multiplet is chosen to obey Dirichlet boundary conditions. In total, the conditions are

$$\begin{cases} A_4^{SO(2N+2)}|_{x^4=0} = 0 = \partial_4 A_\mu^{SO(2N+2)}|_{x^4=0} \\ A_\mu^{SO(2N+2)\setminus H}|_{x^4=0} = 0 \\ \Phi^{SO(2N+2)}|_{x^4=0} = 0 \end{cases} \quad \text{for } \mu = 0, 1, 2, 3. \quad (3.27)$$

Obviously, such boundary condition on the gauge multiplet turn out to be $\frac{1}{2}$ BPS and as such preserve half of 5d $\mathcal{N} = 1$ supersymmetries.

Boundary conditions for punctures. So far, non-maximal boundary conditions have been discussed for the domain wall. However, one needs to defined the boundary conditions for punctures with non-maximal symmetry as well. Suppose the construction contains a non-maximal open puncture with symmetry group H , then, as customary in the literature [6, 7], one reverses the

above boundary conditions on the gauge multiplet, i.e.

$$\begin{cases} A_\mu^{SO(2N+2)}|_{x^4=0} = 0 \\ \Phi^{SO(2N+2)\setminus H}|_{x^4=0} = 0 = \partial_4 \Phi^{H\subset SO(2N+2)}|_{x^4=0} \end{cases} \quad \text{for } \mu = 0, 1, 2, 3, 4. \quad (3.28)$$

Such non-maximal boundary conditions imply that the punctures have a reduced global symmetry H . The non-zero components of the adjoint chiral Φ^H induces a negative anomaly inflow contribution from the 5d quiver theory to the 4d domain wall due to the H -puncture. Similar non-maximal boundary conditions can be also applied to the $SO(2N+2)$ gauge nodes in the 5d quiver (3.1) with $(N-1)$ attached hypermultiplets. This becomes relevant at the end of this section.

$SU(N)$ - $USp(2N-2)$ domain wall. In order to construct a domain wall with $SU(N)$ - $USp(2N-2)$ puncture symmetry, in contrast to the maximal boundary conditions (3.5) and (3.8), one only imposes $\frac{1}{2}$ BPS boundary conditions for the first N hypermultiplets of the $USp(2N-2)$ node

$$+) \quad \partial_4 X_i|_{x^4=0} = Y_i|_{x^4=0} = 0, \quad \text{or} \quad -) \quad X_i|_{x^4=0} = \partial_4 Y_i|_{x^4=0} = 0, \quad \text{for } i = 1, 2, \dots, N, \quad (3.29a)$$

while the remaining hypermultiplets are forced to vanish, i.e.

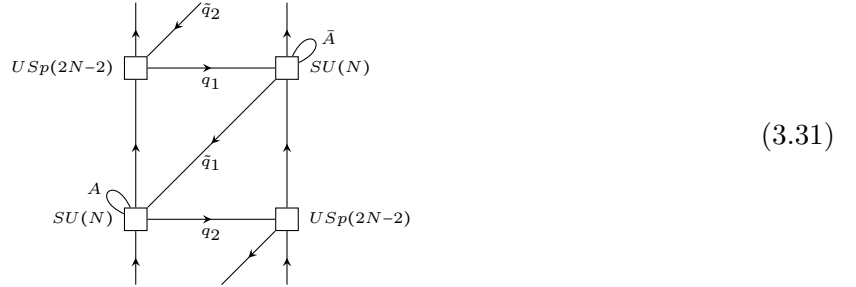
$$X_{N+1} = Y_{N+1} = 0. \quad (3.29b)$$

Correspondingly, one also has to reduce the rank of gauge group via suitable vector multiplet boundary conditions,

$$\begin{cases} A_4^{SO(2N+2)}|_{x^4=0} = 0 = \partial_4 A_\mu^{SO(2N+2)}|_{x^4=0} \\ A_\mu^{SO(2N+2)\setminus SU(N)}|_{x^4=0} = 0 \end{cases} \quad \text{for } \mu = 0, 1, 2, 3. \quad (3.30)$$

The adjoint chiral field is subjected to Dirichlet boundary conditions as above.

Starting, for instance, from (3.17), these non-maximal boundary conditions allow to obtain the following modified domain wall with $SU(N)$ - $USp(2N-2)$ punctures:



One can verify explicitly that all $\text{Tr}(U(1)_R G^2)$ anomalies vanish. Of course, with this modification, one would worry about the cubic anomaly of the $SU(N)$ nodes. However, as explained in previous sections, one can always glue two cubic anomalous domain walls with opposite cubic anomalies to render the $SU(N)$ node anomaly free.

$SO(2N+2)$ - $SU(N-1)$ domain wall. Similarly for a $SO(2N+2)$ - $SU(N-1)$ domain wall, see for example (3.20), one computes a non-vanishing $\text{Tr}(U(1)_R G^2)$ anomaly for $G = SO(2N+2)$, i.e.

$$\text{Tr}(U(1)_R SO(2N+2)^2) = (0-1) \cdot (N-1) + \frac{1}{2}(2N+2-2) = +1. \quad (3.32)$$

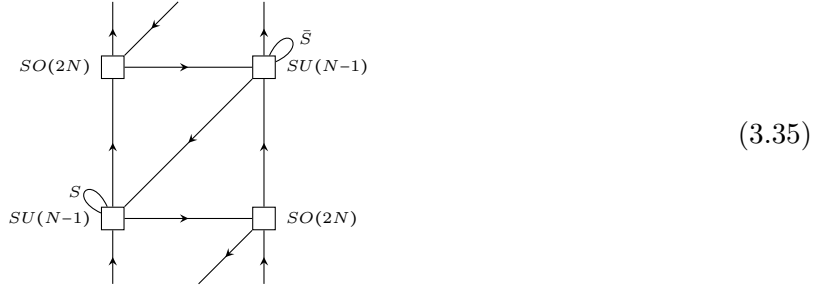
If one considers a $SO(2N+2)$ - $SU(N)$ domain wall instead, one finds

$$\text{Tr} (U(1)_R SO(2N+2)^2) = 0 = \text{Tr} (U(1)_R SU(N)^2). \quad (3.33)$$

However, $SU(N)$ cannot be embedded into $USp(2N-2)$. This suggests to consider a *smaller puncture* by assigning non-maximal $\frac{1}{2}$ BPS boundary conditions on the vector multiplet for only a subgroup $SO(2N) \subset SO(2N+2)$,

$$\begin{cases} A_4^{SO(2N+2)}|_{x^4=0} = 0 = \partial_4 A_\mu^{SO(2N+2)}|_{x^4=0} \\ A_\mu^{SO(2N+2) \setminus SO(2N)}|_{x^4=0} = 0 \end{cases} \quad \text{for } \mu = 0, 1, 2, 3, \quad (3.34)$$

such that a domain wall with puncture symmetry $SO(2N)$ - $SU(N-1)$ arises, i.e.



For completeness, (3.34) is supplemented by Dirichlet boundary condition for the adjoint-valued chiral in the $SO(2N+2)$ vector multiplet.

Mixed domain wall. Lastly, for the mixed domain wall (3.23), one finds that the vanishing $\text{Tr} (U(1)_R G^2)$ anomaly constraints for all $G = USp, SO, SU$ require to further reduce the $USp(2N-2) - SU(N)$ puncture symmetry of the quiver (3.21) to $USp(2N-4) - SU(N-1)$. To do so, on the left chamber, one assigns $\frac{1}{2}$ BPS boundary conditions on the vector multiplet for only a subgroup $USp(2N-4) \subset USp(2N-2)$, i.e.

$$\begin{cases} A_4^{USp(2N-2)}|_{x^4=0} = 0 = \partial_4 A_\mu^{USp(2N-2)}|_{x^4=0} \\ A_\mu^{USp(2N-2) \setminus USp(2N-4)}|_{x^4=0} = 0 \\ \Phi^{USp(2N-2)}|_{x^4=0} = 0 \end{cases}, \quad \text{for } \mu = 0, 1, 2, 3, \quad (3.36a)$$

$$\begin{cases} A_4^{SO(2N+2)}|_{x^4=0} = 0 = \partial_4 A_\mu^{SO(2N+2)}|_{x^4=0} \\ A_\mu^{SO(2N+2) \setminus SU(N-1)}|_{x^4=0} = 0 \\ \Phi^{SO(2N+2)}|_{x^4=0} = 0 \end{cases}, \quad \text{for } \mu = 0, 1, 2, 3. \quad (3.36b)$$

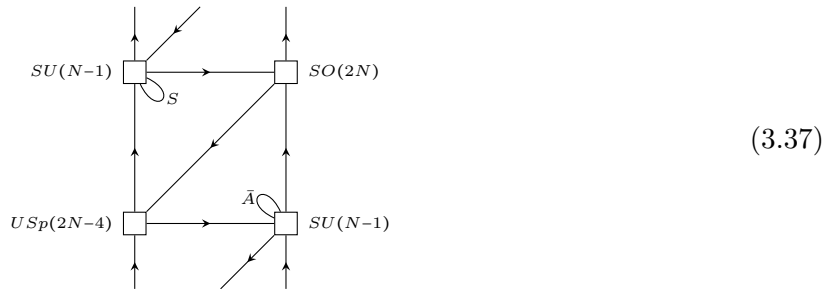
In addition, $\frac{1}{2}$ BPS boundary conditions are imposed for the first $(N-1)$ hypermultiplets

$$+) \quad \partial_4 X_i|_{x^4=0} = Y_i|_{x^4=0} = 0, \quad \text{or} \quad -) \quad X_i|_{x^4=0} = \partial_4 Y_i|_{x^4=0} = 0, \quad \text{for } i = 1, 2, \dots, N-1, \quad (3.36c)$$

while Dirichlet boundary conditions are imposed on the remaining two hypermultiplets

$$X_N = Y_N = X_{N+1} = Y_{N+1} = 0. \quad (3.36d)$$

On the right chamber, the boundary conditions are assigned to be the same as in (3.34). The resulting domain wall is



In total, there are still three types of domain walls, but the puncture symmetries have changed to $USp(2N-4)$ - $SU(N-1)$ and $SO(2N)$ - $SU(N-1)$. These domain walls are equipped with a non-anomalous $U(1)_R \subset SU(2)_R$ symmetry, i.e.

$$\text{Tr} \left(U(1)_R USp(2N-4)^2 \right) = \text{Tr} \left(U(1)_R SO(2N)^2 \right) = \text{Tr} \left(U(1)_R SU(N-1)^2 \right) = 0, \quad (3.38)$$

with $U(1)_R$ -charge assignments as in Table 1. In addition, computing the $U(1)_R$ -gravity anomalies reveals that

$$\text{Tr} \left(U(1)_R \right) = 0 = \text{Tr} \left(U(1)_R^3 \right), \quad (3.39)$$

holds for all three domain walls. It implies that for a quiver theory, constructed from glueing these domain walls on a torus, the $U(1)_R$ symmetry is preserved and the $U(1)_R$ -gravity anomalies vanish. Consequently, there is a possibility that such 4d quiver theories have a 6d origin. Despite the intermediate success of constructing sensible theories via domain walls, the necessity of non-maximal boundary conditions opens the door to a partial loss of information from the 6d origin. In the next section, the 4d theories constructed from non-maximal boundary conditions will be considered in detail.

4 Four dimensions

In this section, the 4d theories are constructed via domain walls that arise from non-maximal boundary conditions.

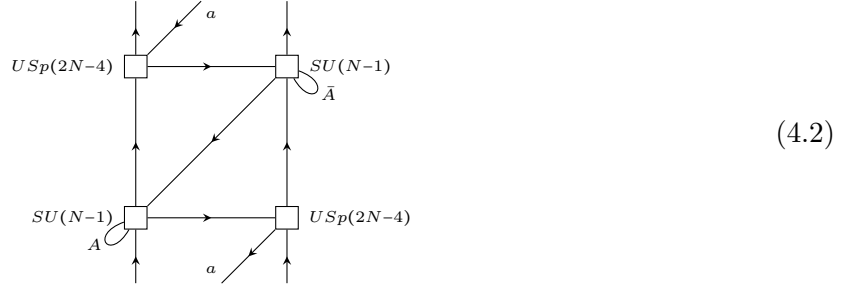
4.1 Domain wall for non-maximal boundary conditions

Here an example made of USp -mixed- SO -mixed domain walls is presented, which satisfies the criteria

$$\text{Tr} \left(U(1)_R \right) = 0 = \text{Tr} \left(U(1)_R^3 \right) \quad (4.1)$$

with non-zero a -central charge.

$USp(2N-4)$ - $SU(N-1)$ domain wall. Collecting all the ingredients, the domain wall becomes



where A, \bar{A} denote chiral supermultiplets in the anti-symmetric representation and its conjugate. Being careful, one should analyse various anomalies. Firstly, for the cubic anomalies of the left and right $SU(N)$ groups, one finds

$$\text{Tr}(SU(N)_L^3) = -(2N-4) + (N-1) + (N-5) = -2, \quad (4.3a)$$

$$\text{Tr}(SU(N)_R^3) = +(2N-4) - (N-1) + (N-5) = +2. \quad (4.3b)$$

Secondly, to compute $U(1)_R$ anomalies of the four nodes, one needs to clarify the R -charge assignment. Following the discussion of the last sections, i.e. the R -charge of all vertical lines is 1, and horizontal lines have R -charge 0. Hence, the superpotential imposes that diagonal lines and (anti-)symmetric matter fields have their R -charges 1 and 2, respectively. Likewise, the gauge nodes contribute as $\frac{1}{2}$ of the 4d gauginos' anomaly contribution with R -charge 1, due to 5d anomaly inflow. Then, one computes

$$\text{Tr}(U(1)_R USp(2N-4)_L^2) = (0-1) \cdot (N-1) + \frac{1}{2} \cdot 2(N-1) = 0, \quad (4.4a)$$

$$\text{Tr}(U(1)_R SU(N-1)_L^2) = (0-1) \cdot (2N-4) + (2-1) \cdot (N-3) + \frac{1}{2} \cdot 2(N-1) = 0, \quad (4.4b)$$

$$\text{Tr}(U(1)_R USp(2N-4)_R^2) = (0-1) \cdot (N-1) + \frac{1}{2} \cdot 2(N-1) = 0, \quad (4.4c)$$

$$\text{Tr}(U(1)_R SU(N-1)_R^2) = (0-1) \cdot (2N-4) + (2-1) \cdot (N-4) + \frac{1}{2} \cdot 2(N-1) = 0. \quad (4.4d)$$

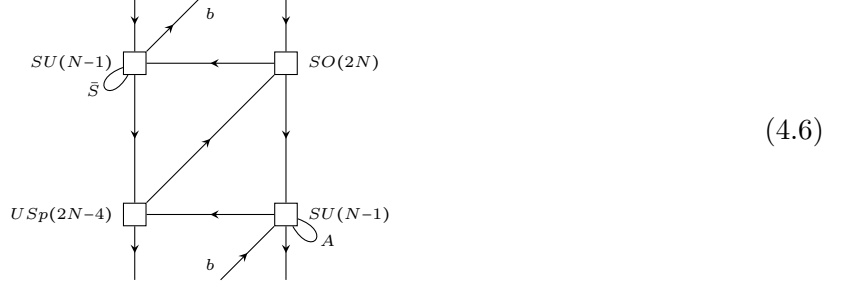
Lastly, computing the $U(1)_R$ -gravity anomalies yields

$$\begin{aligned} \text{Tr}(U(1)_R) = \text{Tr}(U(1)_R^3) = 2 \cdot & \left(-(2N-4) \cdot (N-1) + \frac{1}{2}(N-1)(N-2) \right. \\ & \left. + \frac{1}{2}((N-1)^2 - 1) + \frac{1}{2}(N-2)(2N-3) \right) = 0, \end{aligned} \quad (4.5)$$

where the gaugino contribution is again scaled by a factor of a half.

After these considerations, one can now proceed to glue the domain wall (4.2) from the right or left to some other domain walls with cubic anomalies $+2/-2$ on the left or right side. In order to do so, one needs to introduce other types of domain walls.

Mixed domain wall. The mixed domain wall, meaning that all three types SU , USp , SO of groups are present, is defined as follows:



where \bar{S} is the conjugate of the symmetric representation. Recall that the additional loops have been introduced so that these two domain walls can be S -glued [2]. S -gluing makes all chiral fields corresponding to vertical lines massive and, thus, they can be integrated out. In particular, this will guarantee that all $SO(2N)$ and $USp(2N-4)$ nodes are asymptotically free. The computations of various anomalies is analogous to the above cases, such that one readily obtains

$$\text{Tr}(SU(N-1)_L^3) = +(2N) - (N-1) - (N+3) = -2, \quad (4.7a)$$

$$\text{Tr}(SU(N-1)_R^3) = -(2N-4) + (N-1) + (N-5) = -2, \quad (4.7b)$$

$$\text{Tr}(U(1)_R USp(2N-4)_L^2) = (0-1) \cdot (N-1) + \frac{1}{2} \cdot 2(N-1) = 0, \quad (4.7c)$$

$$\text{Tr}(U(1)_R SU(N-1)_L^2) = (0-1) \cdot 2N + (2-1) \cdot (N+1) + \frac{1}{2} \cdot 2(N-1) = 0, \quad (4.7d)$$

$$\text{Tr}(U(1)_R SO(2N)_R^2) = (0-1) \cdot (N-1) + \frac{1}{2} \cdot 2(N-1) = 0, \quad (4.7e)$$

$$\begin{aligned} \text{Tr}(U(1)_R SU(N-1)_R^2) &= (0-1) \cdot (2N-4) + (2-1) \cdot (N-3) + \frac{1}{2} \cdot 2(N-1) \\ &= 0, \end{aligned} \quad (4.7f)$$

$$\begin{aligned} \text{Tr}(U(1)_R) = \text{Tr}(U(1)_R^3) &= -(2N-4)(N-1) - 2N(N-1) + \frac{1}{2}(N-1)(N-2) \\ &\quad + \frac{1}{2}N(N-1) + 2 \cdot \frac{1}{2}((N-1)^2 - 1) + \frac{1}{2}(N-2)(2N-3) \\ &\quad + \frac{1}{2}N(2N-1) \\ &= 0. \end{aligned} \quad (4.7g)$$

Clearly the domain wall (4.6) with cubic anomaly -2 can be glued to the first USp - SU domain wall (4.2) from the right side. Note in particular that it also a conformal gluing with respect to the $U(1)_R$ symmetry. Next, one has to construct additional domain walls, for instance a SO - SU and another mixed domain wall, such that the domain walls (4.2), (4.6) can be glued to close the torus.

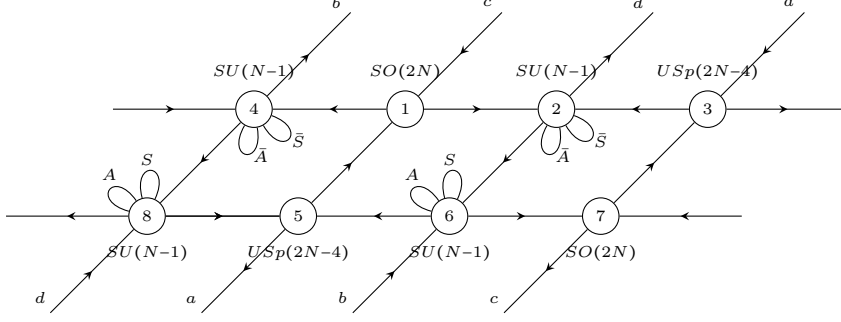
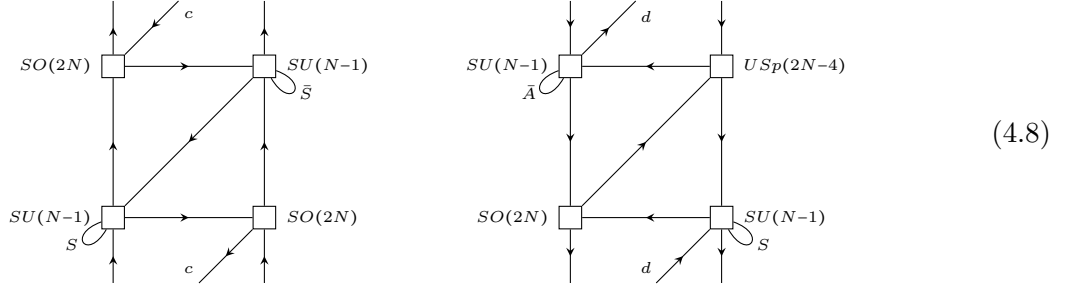


Figure 2: Quiver theory on the torus constructed from the domain walls (4.2), (4.6), and (4.8). The diagonal lines are glued according to the letters a, b, c, d so that every SO or USp node connects to one USp , one SO , and two SU nodes.

SO - SU and mixed domain walls. The remaining possibilities are as follows:



(4.8)

For these two domain walls, one can easily compute the anomalies as before. The SO - SU domain wall has $+2$ and -2 cubic anomaly for the left and right SU gauge node, respectively. The mixed domain wall one has $+2$ cubic anomaly for both SU gauge nodes. All other anomalies vanishes for both domain walls. Therefore, the four domain walls (4.2), (4.6), (4.8) can be conformally glued successively to form a quiver theory on a torus.

4.2 Quiver theory on torus

After consistently gluing all domain walls (4.2), (4.6), (4.8), and integrating all massive vertical fields, one has constructed the quiver theory displayed in Figure 2, which would be understood as placed on a torus. The choice of gluing in Figure 2 is not arbitrary, because the β -functions of the USp and SO nodes are zero up to leading order only on this way of connecting the lines. In more detail, one can straightforwardly compute, using (A.5), that

$$\begin{aligned} \beta_{SO} &= 3 \cdot 2(N-1) - (2(N-1) - 2 + 2(N-1) + 2 + 2(N-1)) + \mathcal{O}(g_{SO}^2) \\ &= 0 + \mathcal{O}(g_{SO}^2), \end{aligned} \quad (4.9a)$$

$$\begin{aligned} \beta_{USp} &= 3 \cdot 2(N-1) - (2(N-1) - 2 + 2(N-1) + 2 + 2(N-1)) + \mathcal{O}(g_{USp}^2) \\ &= 0 + \mathcal{O}(g_{USp}^2). \end{aligned} \quad (4.9b)$$

The β -functions of the SU gauge nodes are positive. From the perturbative analysis based on the β -functions, one would expect that the theory in Figure 2 becomes free in the IR.

Since all four domain walls are conformally glued, the $U(1)_R$ symmetry is preserved. Also, the $U(1)_R$ -gravity anomaly is additive, so for the quiver of Figure 2

$$\text{Tr}(U(1)_R) = \text{Tr}(U(1)_R^3) = 0 \quad (4.10)$$

fields	X_{71}	X_{51}	X_{53}	X_{73}	X_{26}	X_{46}	X_{48}	X_{28}
$U(1)_1$	0	0	0	0	2	0	-2	0
$U(1)_2$	$-\alpha_-^2$	$\alpha_+\alpha_-$	$-\alpha_+^2$	$\alpha_+\alpha_-$	$-4 - \alpha_+\alpha_-$	$\alpha_+\alpha_-$	$-\alpha_+\alpha_-$	$\alpha_+\alpha_-$
fields	q_{12}	q_{32}	q_{34}	q_{14}	q_{85}	q_{65}	q_{67}	q_{87}
$U(1)_1$	α_-	$-\alpha_+$	α_+	$-\alpha_-$	α_+	$-\alpha_+$	α_-	$-\alpha_-$
$U(1)_2$	$-2\alpha_-$	$2\alpha_+$	0	0	0	$2\alpha_+$	$-2\alpha_-$	0
fields	\bar{A}_2	\bar{S}_2	\bar{A}_4	\bar{S}_4	A_6	S_6	A_8	S_8
$U(1)_1$	$2\alpha_+$	$-2\alpha_-$	$-2\alpha_+$	$2\alpha_-$	$2\alpha_+$	$-2\alpha_-$	$-2\alpha_+$	$2\alpha_-$
$U(1)_2$	$-4\alpha_+$	$4\alpha_-$	0	0	$-4\alpha_+$	$4\alpha_-$	0	0

Table 2: Charge assignment of the fields in the quiver gauge theory of Figure 2. Here, $\alpha_{\pm} = \frac{N-1}{2} \pm 1$.

holds. Therefore, the central charge a is zero in the UV regime. However, the RG flow will trigger the UV $U(1)_R$ symmetry to mix with other global $U(1)$ symmetries, such that one has to derive the genuine IR R -symmetry of the theory via a -maximisation [20].

a -maximisation. To begin with, one determines how many non-anomalous global $U(1)$ symmetries exist for the quiver. For bookkeeping, the gauge nodes are numbered, as shown in Figure 2, such that matter fields are labeled by the nodes they connect, see Table 2 for details.

The matter fields carry charges under all compatible global symmetries that are ‘t Hooft anomaly free for each gauge node as well as neutral with respect to the superpotentials. Recall that, besides regular quartic superpotential interactions, there are also superpotential terms for the (anti-)symmetric matter fields. For example, the fields \bar{A}_2 and \bar{S}_2 have superpotential as in (3.19), i.e.

$$\mathcal{W} = q_{12}^2 \bar{S}_2 + q_{32}^2 \bar{A}_2, \quad (4.11)$$

where all indices of these fields are omitted. Carefully evaluating all constraints shows that there are two $U(1)$ flavour symmetries with charges as displayed in Table 2. Having derived the consistent charge assignment, one can proceed to compute the central charge in the IR regime, by defining a trial R -symmetry via

$$R = U(1)_R + x_1 U(1)_1 + x_2 U(1)_2. \quad (4.12)$$

Carrying out the a -maximisation leads to the solution

$$x_1 = x_2 = \frac{2}{3(N-1)^2} \sqrt{\frac{10}{7}}, \quad (4.13)$$

and the central charges a and c are then computed to be

$$a = \frac{5}{3} \sqrt{\frac{10}{7}} \quad \text{and} \quad c = \frac{11}{6} \sqrt{\frac{10}{7}}. \quad (4.14)$$

This central charge is positive, but N -independent. This is an unexpected behaviour from the 6d point of view.

Inspecting the solution (4.13), it follows from Table 2 that for generic values of N

$$\begin{aligned}
-\frac{5}{100} < R_{\text{IR}}(q_{14}, q_{12}, q_{67}, q_{87}) &= -\frac{1}{3} \sqrt{\frac{10}{7}} \frac{N-3}{(N-1)^2} < 0, \\
0 < R_{\text{IR}}(q_{32}, q_{34}, q_{85}, q_{65}) &= \frac{1}{3} \sqrt{\frac{10}{7}} \frac{N+1}{(N-1)^2} < \frac{2}{3},
\end{aligned}
\tag{4.15}$$

while all other fields have IR R -charge above the unitarity bound. In particular, note that zero is a strict bound in (4.15) for any finite N . The (anti-)symmetric chiral fields (and conjugates thereof) have IR R -charges that rapidly approach 2 such that for $N \geq 10$, these are essentially equal to their UV R -charges. Nevertheless, the existence of fundamental fields with R -charge below the unitarity bound requires to carefully consider gauge invariant operators composed of the fields.

Gauge invariant operators and unitarity bound. For the ring of gauge invariant chiral operators (GIO), one can, in principle, compute a generating function [23] by an integral of the form²

$$F_{\text{GIO}} = \prod_a \int \mu_{G_a} \text{PE} \left[\sum_{\text{chirals}} \chi_{\text{chirals}}^G t^{R(\text{chirals})} \right]
\tag{4.16}$$

where the integral is taken over the Haar measures of each group G_a appearing in the gauge group $G = \prod_a G_a$ and the chirals contribute via their group characters χ_{chirals}^G . Hence, F_{GIO} becomes a Laurent series in t , the suitable UV R -charge fugacity. Assuming that the UV R -charges are non-negative, the ring of gauge invariant chiral operators is finitely generated. Consequently, it would be sufficient to analyse IR R -charges of the generating set of gauge invariant operators. However, due to the extensive nature of the quiver theory in Figure 2, this approach is computationally challenging. Instead, an inspection of the quiver reveals the following basic gauge invariants:

- GIOs that do not violate unitarity
 - (i) There are gauge invariant operators which do not violate the unitarity bound. To name a few examples, consider closed loops in the quiver of Figure 2 that obey concatenation of arrows. The so-to-say smallest loops are all given by superpotential terms. By construction, the superpotential terms are of UV R -charge 2 and singlets under the $U(1)_1, U(1)_2$ symmetries. Thus, these gauge-invariant operators have R -charge 2 in the IR.
 - (ii) Gauge invariant operators corresponding to larger closed loops formed by concatenating arrows in the quiver, i.e. not given by a superpotential term, do not violate the unitarity bound either. To see this, it is enough to notice how small the R -charges (4.15) of the unitarity bound violating fields are, and to see that loops necessarily contain vertical chiral fields. The R -charges of these fields are large enough to compensate the small negative R -charges of q_{14}, q_{12}, q_{67} , or q_{87} such that the resulting gauge invariant operator has R -charge above the unitarity bound.
 - (iii) In addition, there are also gauge invariant operators that disobey concatenation of arrows; for instance, the $SO(2N)$ and $USp(2N-4)$ gauge nodes each admit invariant 2-tensors. These give rise to Meson-type operators

$$\delta^{\alpha_7 \beta_7} \delta^{\alpha_1 \beta_1} (X_{71})_{\alpha_7 \alpha_1} (X_{71})_{\beta_7 \beta_1}, \quad \delta^{a_5 b_5} \delta^{a_3 b_3} (X_{53})_{a_5 a_3} (X_{53})_{b_5 b_3},
\tag{4.17}$$

²Note that it is not necessary to consider the chiral ring, i.e. one does not need to quotient by the F-term relations, if one just wants to find the generating set of gauge invariant chiral operators.

where α, β are $SO(2N)$ indices on nodes 1 and 7, while a, b are $USp(2N-4)$ indices on nodes 3 and 5. A calculation then proves that the R -charges of the Meson-type operators are above the unitarity bound. On the other hand, one could consider the Pfaffian for an $SO(2N)$ gauge node which could be constructed as

$$\text{Pf} \left[(q_{67})_{\alpha}^i (A_6)_{[ij]} (q_{67})_{\beta}^j \right] \quad (4.18)$$

where α, β are $SO(2N)$ indices and i, j are $SU(N-1)$ indices. The Pfaffian is then constructed for the antisymmetric $(\alpha\beta)$ indices. However, already the combination of the three chirals has R -charge above the unitarity bound.

- GIOs that do violate unitarity

- (i) There are Baryon-type operators constructed solely from field with negative IR R -charge, i.e.

$$\mathcal{B}_{q_{14}q_{12}} = \varepsilon^{i_1 \dots i_{N-1}} \varepsilon^{j_1 \dots j_{N-1}} (q_{14})_{i_1 \alpha_1} \dots (q_{14})_{i_{N-1} \alpha_{N-1}} \quad (4.19a)$$

$$\cdot (q_{12})_{j_1 \beta_1} \dots (q_{12})_{j_{N-1} \beta_{N-1}} \delta^{\alpha_1 \beta_1} \dots \delta^{\alpha_{N-1} \beta_{N-1}}$$

$$\mathcal{B}_{q_{14}q_{14}} = \varepsilon^{i_1 \dots i_{N-1}} \varepsilon^{j_1 \dots j_{N-1}} (q_{14})_{i_1 \alpha_1} \dots (q_{14})_{i_{N-1} \alpha_{N-1}} \quad (4.19b)$$

$$\cdot (q_{14})_{j_1 \beta_1} \dots (q_{14})_{j_{N-1} \beta_{N-1}} \delta^{\alpha_1 \beta_1} \dots \delta^{\alpha_{N-1} \beta_{N-1}}$$

$$\mathcal{B}_{q_{12}q_{12}} = \varepsilon^{i_1 \dots i_{N-1}} \varepsilon^{j_1 \dots j_{N-1}} (q_{12})_{i_1 \alpha_1} \dots (q_{12})_{i_{N-1} \alpha_{N-1}} \quad (4.19c)$$

$$\cdot (q_{12})_{j_1 \beta_1} \dots (q_{12})_{j_{N-1} \beta_{N-1}} \delta^{\alpha_1 \beta_1} \dots \delta^{\alpha_{N-1} \beta_{N-1}}$$

with the $SO(2N)$ indices $\alpha, \beta \in \{1, 2, \dots, 2N\}$ and the $SU(N-1)$ indices $i, j \in \{1, 2, \dots, N-1\}$. By the same reasoning, one constructs the GIOs $\mathcal{B}_{q_{67}q_{87}}$, $\mathcal{B}_{q_{67}q_{67}}$, $\mathcal{B}_{q_{87}q_{87}}$. Besides these generalised Baryons, one may reconsider Pfaffian-type invariants of the form

$$\mathcal{P}_{q_{12}q_{14}} = \text{Pf} \left[\left(\varepsilon^{i_1 \dots i_{N-1}} \varepsilon^{j_1 \dots j_{N-1}} (q_{14})_{i_1 \alpha_1} \dots (q_{14})_{i_{N-1} \alpha_{N-1}} \cdot (q_{12})_{j_1 \beta_1} \dots (q_{12})_{j_{N-1} \beta_{N-1}} \delta^{\alpha_2 \beta_2} \dots \delta^{\alpha_{N-1} \beta_{N-1}} \right)_{\alpha_1 \beta_1} \right] \quad (4.20)$$

where the $SO(2N)$ Pfaffian is constructed from the anti-symmetric part in the α_1, β_1 indices. Likewise, the Pfaffian $\mathcal{P}_{q_{67}q_{87}}$ can be constructed. Then (4.15) implies

$$R_{\text{IR}}(\mathcal{B}_{q_{14}q_{12}}, \mathcal{B}_{q_{14}q_{14}}, \mathcal{B}_{q_{12}q_{12}}, \mathcal{B}_{q_{67}q_{87}}, \mathcal{B}_{q_{67}q_{67}}, \mathcal{B}_{q_{87}q_{87}}, \mathcal{P}_{q_{12}q_{14}}, \mathcal{P}_{q_{67}q_{87}}) < 0. \quad (4.21)$$

- (ii) Apart from gauge invariant operators constructed from fundamental chirals with negative R -charge, one can also consider operators with positive R -charge below the unitarity bound as long as enough q_{12} , q_{14} , q_{67} , q_{87} are involved. As example, considered the following GIO:

$$\mathcal{O}_{q_{14}q_{12}}^{(1)} = J^{ab} (q_{34})_{i_1 a} (q_{32})_{j_1 b} \varepsilon^{i_1 \dots i_{N-1}} \varepsilon^{j_1 \dots j_{N-1}} (q_{14})_{i_2 \alpha_2} \dots (q_{14})_{i_{N-1} \alpha_{N-1}} \quad (4.22a)$$

$$\cdot (q_{12})_{j_2 \beta_2} \dots (q_{12})_{j_{N-1} \beta_{N-1}} \delta^{\alpha_2 \beta_2} \dots \delta^{\alpha_{N-1} \beta_{N-1}}$$

which can be generalised to $l = 1, 2, \dots, N-1$

$$\mathcal{O}_{q_{14}q_{12}}^{(l)} = J^{a_1 b_1} (q_{34})_{i_1 a_1} (q_{32})_{j_1 b_1} \dots J^{a_l b_l} (q_{34})_{i_l a_l} (q_{32})_{j_l b_l} \quad (4.22b)$$

$$\varepsilon^{i_1 \dots i_{N-1}} \varepsilon^{j_1 \dots j_{N-1}} (q_{14})_{i_{l+1} \alpha_{l+1}} \dots (q_{14})_{i_{N-1} \alpha_{N-1}} \cdot (q_{12})_{j_{l+1} \beta_{l+1}} \dots (q_{12})_{j_{N-1} \beta_{N-1}} \delta^{\alpha_{l+1} \beta_{l+1}} \dots \delta^{\alpha_{N-1} \beta_{N-1}}$$

with the $USp(2N-4)$ indices $a, b \in \{1, 2, \dots, 2N-4\}$. Similarly, one also finds

$$\begin{aligned} \tilde{\mathcal{O}}_{q_{14}q_{12}}^{(1)} = & J^{ab}(q_{34})_{i_1 a}(q_{34})_{i_2 b} \varepsilon^{i_1 \dots i_{N-1}}(q_{14})_{i_3 \alpha_3} \dots (q_{14})_{i_{N-1} \alpha_{N-1}} \\ & \cdot J^{cd}(q_{32})_{j_1 c}(q_{32})_{j_2 d} \varepsilon^{j_1 \dots j_{N-1}}(q_{12})_{j_3 \beta_3} \dots (q_{12})_{j_{N-1} \beta_{N-1}} \delta^{\alpha_3 \beta_3} \dots \delta^{\alpha_{N-1} \beta_{N-1}} \end{aligned} \quad (4.23a)$$

and generalisations thereof

$$\begin{aligned} \tilde{\mathcal{O}}_{q_{14}q_{12}}^{(l)} = & J^{a_1 b_1}(q_{34})_{i_1 a_1}(q_{34})_{i_2 b_1} \dots J^{a_l b_l}(q_{34})_{i_{2l-1} a_l}(q_{34})_{i_{2l} b_l} \\ & \cdot \varepsilon^{i_1 \dots i_{N-1}}(q_{14})_{i_{2l+1} \alpha_{2l+1}} \dots (q_{14})_{i_{N-1} \alpha_{N-1}} \\ & \cdot J^{c_1 d_1}(q_{32})_{j_1 c_1}(q_{32})_{j_2 d_1} \dots J^{c_l d_l}(q_{32})_{j_{2l-1} c_l}(q_{32})_{j_{2l} d_l} \\ & \cdot \varepsilon^{j_1 \dots j_{N-1}}(q_{12})_{j_3 \beta_2} \dots (q_{12})_{j_{N-1} \beta_{N-1}} \delta^{\alpha_{2l+1} \beta_{2l+1}} \dots \delta^{\alpha_{N-1} \beta_{N-1}}. \end{aligned} \quad (4.23b)$$

From Table 2 and the solution (4.13), one finds

$$R_{\text{IR}} \left(\mathcal{O}_{q_{14}q_{12}}^{(l)} \right) = \frac{2}{3} \sqrt{\frac{10}{7}} \cdot \frac{3+2l-N}{N-1} < 0 \quad \text{for } 2l < N-3, \quad (4.24a)$$

$$R_{\text{IR}} \left(\tilde{\mathcal{O}}_{q_{14}q_{12}}^{(l)} \right) = \frac{2}{3} \sqrt{\frac{10}{7}} \cdot \frac{3+4l-N}{N-1} < 0 \quad \text{for } 4l < N-3, \quad (4.24b)$$

such that the R -charge is smaller than $\frac{2}{3}$ for large enough N . Analogously, one defines the operators $\mathcal{O}_{q_{67}q_{87}}^{(l)}$ and $\tilde{\mathcal{O}}_{q_{67}q_{87}}^{(l)}$.

(iii) As a last example, one can even construct unitarity violating operators by combining the q_{12} , q_{14} , q_{67} , q_{87} with some of the vertical fields. For instance

$$\begin{aligned} \mathcal{O} = & \varepsilon^{i_1 \dots i_{N-1}} \varepsilon^{j_1 \dots j_{N-1}} (q_{14})_{i_1 \alpha_1} \dots (q_{14})_{i_{N-1} \alpha_{N-1}} (q_{12})_{j_1 \beta_1} \dots (q_{12})_{j_{N-1} \beta_{N-1}} \delta^{\alpha_2 \beta_2} \dots \delta^{\alpha_{N-1} \beta_{N-1}} \\ & \cdot \varepsilon_{k_1 \dots k_{N-1}} \varepsilon_{l_1 \dots l_{N-1}} (q_{67})_{\rho_1}^{k_1} \dots (q_{67})_{\rho_{N-1}}^{k_{N-1}} (q_{87})_{\sigma_1}^{l_1} \dots (q_{87})_{\sigma_{N-1}}^{l_{N-1}} \delta^{\rho_2 \sigma_2} \dots \delta^{\rho_{N-1} \sigma_{N-1}} \\ & \cdot (X_{71})^{\alpha_1 \rho_1} (X_{71})^{\beta_1 \sigma_1} \end{aligned} \quad (4.25)$$

which has R -charge given by

$$R_{\text{IR}}(\mathcal{O}) = \frac{42 - 5\sqrt{70}}{21} + \frac{12\sqrt{70}}{21(N-1)} - \frac{4\sqrt{70}}{21(N-1)^2}. \quad (4.26)$$

For large enough N , the operator \mathcal{O} violates the unitarity bound.

Consequently, GIOs below the unitarity bound need to be taken care of. Following the discussion in [24], one would conclude that such gauge-invariant operators become free somewhere in the RG-flow and decouple. Hence, their contribution to the a -maximisation has to be subtracted in order to focus on the (potentially) interacting SCFT. As proposed in [25], this can be realised by introducing a *flip field* $\beta_{\mathcal{O}}$ for a unitarity violating gauge invariant operator \mathcal{O} such that

- (i) $\beta_{\mathcal{O}}$ is a gauge singlet, and
- (ii) $\beta_{\mathcal{O}}$ couples via the superpotential term $\mathcal{W} \sim \beta_{\mathcal{O}} \mathcal{O}$.

Performing an a -maximisation with flip-fields for all the unitarity violating GIOs discussed above, leads to an IR R -charge assignment where also X_{71} , X_{53} , X_{26} , X_{48} have negative R -charges. As a consequence, many more GIOs fall below the unitarity bound and would need to be taken care of.

The appearing problem of unitarity-violating GIOs seems to be linked with the positivity of the β -functions (4.9). The expectation is that the theory becomes free in the IR; therefore, it is suggestive to interpret the appearance of the large number of non-unitary GIOs at each iteration of the a -maximisation as indication that the process only terminates after all GIOs are removed from the theory. Hence, the theory would become free in the IR.

Multiple layers. The construction that led to the quiver theory of Figure 2 can be repeated to have more layers. In other words, gluing several copies along the legs labeled a, b, c, d . Thorough analysis of the anomaly and superpotential constraints for $k = 2, 3, 4$ layers reveals that there exist three non-anomalous global $U(1)$ symmetries. As a non-trivial consistency check of the calculation, one verifies that $\text{Tr}(U(1)_R) = \text{Tr}(U(1)_R^3) = 0$ in the UV. Performing a -maximisation with respect to these three global $U(1)$ symmetries, one finds

$$a_{k \text{ layers}} = k \cdot \frac{5}{3} \sqrt{\frac{10}{7}} \quad \text{and} \quad c_{k \text{ layers}} = k \cdot \frac{11}{6} \sqrt{\frac{10}{7}}. \quad (4.27)$$

As in the single layer case, one finds several gauge-variant chiral fields that violate unitarity. In more detail, essentially all horizontal chirals are below the unitarity; in particular, horizontal chirals transforming as bifundamentals of some $SU(N-1)$ and $SO(2N)$ have negative IR R -charge. Repeating the discussion of the single layer case reveals an increasingly large number of unitarity-violating GIOs which would need to be taken care of. Again, this is taken as indication that the multiple layer theory becomes free in the IR, in agreement with the expectation from the β -function analysis (4.9). As a consistence check, the multiple layer analysis confirms the behaviour studied in detail in the single layer case.

4.3 Quiver theory on 2-punctured sphere

Besides the theory on the torus, one can also attempt to study a meaningful 4d theory on a two-punctured sphere. Analogously to the theory on the 2-torus, two perspectives are taken: (i) the compactification of the 6d theory (2.1) on a 2-punctured sphere with fluxes, and (ii) construction via fundamental domain walls on the tube glued together with suitable punctures.

4.3.1 6d theory on 2-punctured sphere

Recall the anomaly 6-form (2.20) for the compactification on a 2-sphere with s punctures and specialise to $s = 2$. Proceeding to a -maximisation as in Section 2.4, one observes that there are no changes to the trace contributions which one reads off from the anomaly polynomial. Hence, (2.24) are valid for the two-punctured 2-sphere and the a -maximisation proceeds as in the T^2 case. In particular, the solutions found in (2.25), (2.26), (2.27) remain valid, but the a -central charge needs to be adjusted. As elaborated in [2, 7], the puncture contribution is intimately linked to the 5d theory resulting from putting the 6d theory on a circle [10]. The 5d $\mathcal{N} = 1$ theory (3.1) is composed of k $SO(2N+2)$ and k $USp(2N-2)$ nodes and the additional anomaly inflow contributions modify $\text{Tr}(R_{IR})$ and $\text{Tr}(R_{IR}^3)$, i.e.

$$\begin{aligned} \text{Tr}(R_{\text{punct.}}) &= \text{Tr}(R_{\text{punct.}}^3) = -\frac{s}{2} \cdot k \cdot (\dim(SO(2N+2)) + \dim(USp(2N-2))) \\ &= -s \cdot k(2N^2 - 1), \end{aligned} \quad (4.28)$$

$$\Rightarrow a_{S^2} = a_{T^2} - \frac{3s}{16} k(2N^2 + 1), \quad (4.29)$$

which relies on the assumption that the maximal symmetry in 5d is realised.

On the other hand, if the punctures do not exhibit the full symmetry, but subgroups $H_{SO} \subset SO(2N+2)$ and $H_{Sp} \subset USp(2N-2)$, respectively, then the boundary conditions are chosen as in (3.28). The anomaly inflow contributions, which originate from the 5d $U(1)_R$ CS-term for the non-trivial $H_{Sp,SO}$ components of the adjoint chiral, change accordingly to

$$\text{Tr}(R_{\text{punct.}}) = \text{Tr}(R_{\text{punct.}}^3) = -\frac{s}{2} \cdot k \cdot (\dim(H_{SO}) + \dim(H_{Sp})). \quad (4.30)$$

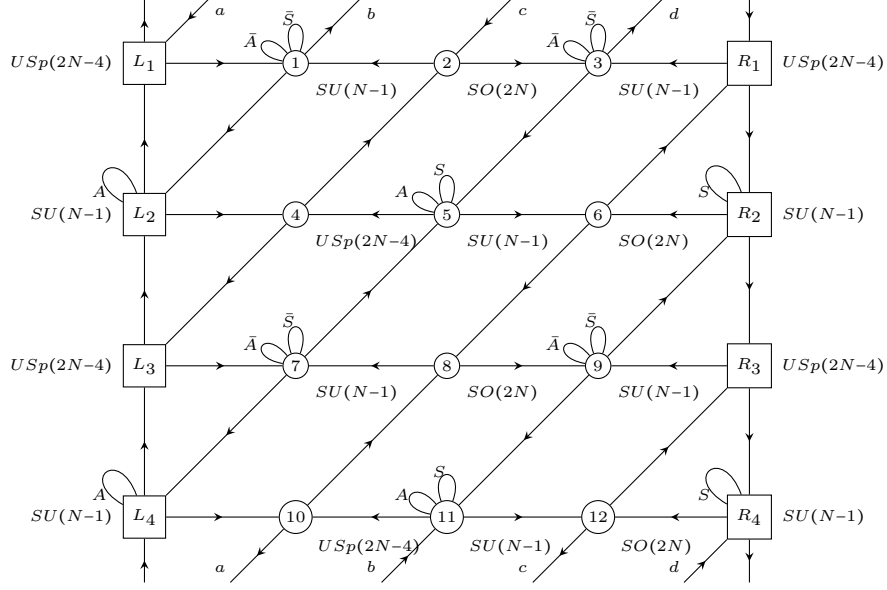


Figure 3: A quiver theory on a two-punctures sphere, for $k = 2$. The theory is constructed from the domain walls (4.2), (4.6), and (4.8), but it is not glued to a torus. As for the torus theory of Figure 2, the diagonal lines are identified according to the labels a, b, c, d .

Suppose $H_{SO,Sp}$ are the maximal subgroups preserving the rank, $H_{SO} = SU(N+1)$ and $H_{Sp} = SU(N-1)$, then one finds

$$\text{Tr}(R_{\text{punct.}}) = \text{Tr}(R_{\text{punct.}}^3) = -s \cdot kN^2 \quad (4.31)$$

$$\Rightarrow a_{S_s^2} = a_{T^2} - \frac{3s}{16}kN^2. \quad (4.32)$$

4.3.2 Quiver theory from domain walls

As an example, consider the theory in Figure 3 where the two punctures each have symmetry $USp(2N-4)^2 \times SU(N-1)^2$. From the quiver diagram, one straightforwardly derives that there are 8 anomaly-free $U(1)$ flavour symmetries. Subsequently performing a -maximisation with respect to all of them leads to an a -central charge behaving as displayed in Figure 4.

Gauge invariant operators and unitarity bound. After the a -maximisation of the theory in Figure 3, one has to inspect the IR R -charges again. Similar to the theory on the torus, one can summarise the numerical results as follows:

$$-\frac{1}{2} \leq R_{IR}(q_{21}, q_{23}, q_{87}, q_{89}) < 0, \quad 0 \leq R_{IR}(\text{other horizontal } q) < \frac{2}{3}, \quad (4.33a)$$

$$R_{IR}(\text{(anti-)symmetric chirals } A, S) > 1, \quad (4.33b)$$

$$R_{IR}(\text{boundary fields } Y) > \frac{2}{3}, \quad (4.33c)$$

$$\frac{1}{2} \leq R_{IR}(X_{6R_1}, X_{12R_3}, X_{4L_3}, X_{10L_1}) < \frac{2}{3}, \quad R_{IR}(\text{other vertical } X) > \frac{2}{3}. \quad (4.33d)$$

Again, the existence of gauge variant objects violating unitarity by itself is not problematic, but one needs to consider all gauge invariant operators carefully. As in the Section 4.2, it is sufficient

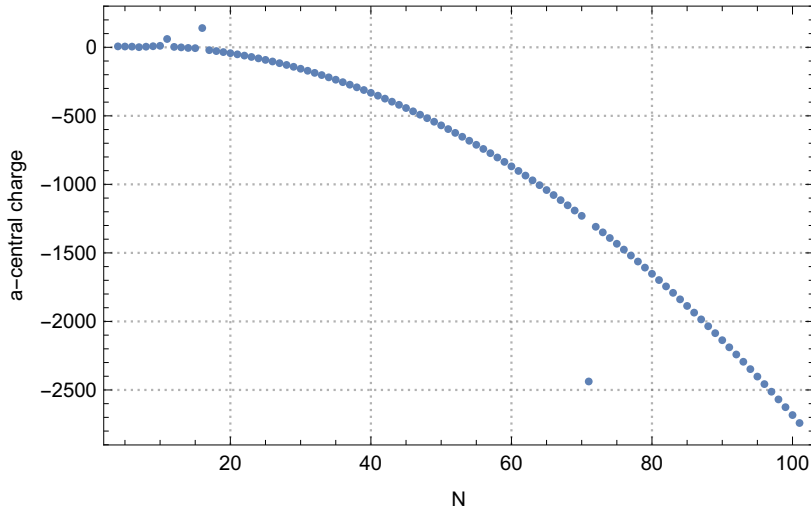


Figure 4: The numerical results of the a -maximisation: the central charge is displayed against varying rank N of the gauge nodes. Note that the numerical results for $N = 12, 16, 71$ seem to be flawed.

to focus on invariants build from unitarity violating chirals. It is immediate that some unitarity violating operators of the quiver theory in Figure 2 are also unitarity violating GIOs in the theory of Figure 3; for instance, the analogs of the Baryon-type operators (4.19) and Pfaffian-type operators (4.20) for $q_{21}, q_{23}, q_{87}, q_{89}$ do exist. In addition, compared to the quiver on the torus of Figure 2, the conceptually new gauge invariant operators are the following:

- (i) Since the quiver has flavour nodes, some gauge invariant operators can originate from paths starting and ending on a flavour node. For instance,

$$(X_{7L4})_i^{m7} (q_{87})_{am7} \delta^{ab} (q_{89})_{bn9} (X_{9R2})_j^{n9} \quad (4.34)$$

where the $SO(2N)$ gauge indices are contracted by the invariant tensor of SO . However, this operator does not violate unitarity. More generally, paths flavour nodes that originate from concatenation of arrows do not introduce unitarity violating operators, because the R -charges of the involved horizontal and (anti-)symmetric chirals are large enough.

- (ii) Meson-type operators for horizontal chirals that transform under an $SO(2N)$ gauge node and an $SU(N-1)$ flavour node lead to operators violating the unitarity bound. For instance,

$$\mathcal{M}_{R_2}^{(i,j)} = \sum_{a,b=1}^{2N} \delta^{ab} (q_{R_2 6})_a^i (q_{R_2 6})_b^j, \quad \mathcal{M}_{R_4}^{(i,j)} = \sum_{a,b=1}^{2N} \delta^{ab} (q_{R_4 12})_a^i (q_{R_4 12})_b^j, \quad (4.35a)$$

which both transform in the 2nd-rank symmetric product of the anti-fundamental representation of an $SU(N-1)$ flavour group. Similarly, Mesons constructed from chirals that transform under an $USp(2N-4)$ gauge node and an $SU(N-1)$ flavour node lead to problematic gauge invariant operators.

$$\mathcal{M}_{L_2}^{[i,j]} = \sum_{\alpha,\beta=1}^{2N-4} J^{\alpha\beta} (q_{L_2 4})_\alpha^i (q_{L_2 4})_\beta^j, \quad \mathcal{M}_{L_4}^{[i,j]} = \sum_{\alpha,\beta=1}^{2N-4} J^{\alpha\beta} (q_{L_4 10})_\alpha^i (q_{L_4 10})_\beta^j, \quad (4.35b)$$

which transform in the 2nd-rank anti-symmetric product of the anti-fundamental representation of some $SU(N-1)$ flavour group.

Again, the non-unitary GIOs are expected to become free somewhere on the RG-flow and decouple [24]. Then the a -maximisation is modified by suitable flip fields [25]. Inspecting the theory in

Figure 3 reveals that (anti-)symmetric chirals S_{R_6} , S_{R_2} , A_{L_2} , and A_{L_4} of the $SU(N-1)$ flavour nodes serves as flip fields for the Meson operators (4.35), because of couplings like (4.11). Since, the flip fields have been included in the a -maximisation, the Meson-type operators are already removed. However, one still has to take care of all the non-unitary GIOs that descend from the quiver on the torus. Analogously to the discussion in Section 4.2, introducing all relevant flip fields, and re-perform a -maximisation is expected to yield even more GIOs below the unitarity bound, such that the theory in Figure 3 is anticipated to become free in the IR.

5 Conclusions

In this paper we explored compactifications of 6d D -type $(1,0)$ SCFTs on the torus and to some extent on the two-punctured sphere preserving 4d $\mathcal{N} = 1$ superconformal symmetry. We explicitly computed the 4d central charges by integrating the anomaly polynomial of the 6d theory turning on fluxes and determined their values in the deep IR using a -maximisation. We observe an interesting $N^{3/2}$ growth of these central charges where $N+1$ is the rank of our D -type quiver. The second part of the paper dealt with explicit constructions of candidate 4d UV Lagrangians arising from such 6d compactifications. Here we found that anomaly considerations at the level of the 4d Lagrangian theory impose severe constraints on the gauge nodes and the matter content. We find that within our framework only non-maximal boundary conditions turn out to be consistent. In particular, we note that imposing UV R -charge assignments determined by 5d domain wall constructions uniquely singles out non-maximal boundary conditions, which are novel and should be explored further. However, the constructed 4d quiver theories appear to be IR free, which is indicated from two directions. On the one hand, the β -functions are positive. On the other hand, the a -maximisation is spoiled by a large number of unitarity-violating gauge invariant operators. We expect that the process of introducing flip fields and re-performing a -maximisation only terminates once the free IR theory is reached.

In view of the 6d prediction, the mismatch is not utterly surprising. Firstly, boundary conditions for orthogonal and symplectic gauge groups have not been thoroughly studied, yet. Secondly, non-maximal boundary conditions have not been explored from the point of view of anomalies even for 6d parent theories of A -type. Thirdly, the anomaly polynomial has no information on potentially unitarity-violating operators or free operators. We expect that accounting correctly for these effects will correct the $N^{3/2}$ -dependence of the a -central charge in 4d.

We postpone a more detailed study for future work.

Acknowledgements. We are grateful to Shlomo S. Razamat for discussions and useful suggestions in the early stage of this work. We would like to express our gratitude towards the referee whose thorough comments helped to improve this paper. The research of J.C. is supported in part by the Chinese Academy of Sciences (CAS) Hundred-Talent Program and by Projects No. 11747601 and No. 11535011 supported by National Natural Science Foundation of China. The work of B.H. and M.S. was supported by the National Thousand-Young-Talents Program of China.

A Notations, anomalies and β -functions

This appendix provides a summary of the group theoretical notations, and a brief review of various 't Hooft anomalies and NSVZ β -functions. Following for instance [26], all required group theoretical constants and conventions are collected in Table 3. For convenience, the formulae for various anomalies are recalled.

G	$SU(N)$	$USp(2N-2)$	$SO(2N+2)$
r_G	$N-1$	$N-1$	$N+1$
h_G^\vee	N	N	$2N$
d_G	N^2-1	$(N-1)(2N-1)$	$(N+1)(2N+1)$
$t_2(\text{fund.})$	1	1	1
$t_2(\text{adj.})$	$2N$	$2N$	$2N$
$t_2(\text{sym.})$	$N+2$	$-$	$-$
$t_2(\text{antisym.})$	$N-2$	$-$	$-$
$A(\text{fund.})$	1	0	0
$A(\text{sym.})$	$N+4$	0	0
$A(\text{antisym.})$	$N-4$	0	0

Table 3: Group theoretical constants. Here, r_G denotes for the rank, d_G is the dimension of G , and h_G^\vee is the dual Coxeter number. For a given representation of a group G , $t_2(\text{rep.})$ denotes the second Dynkin index, while $A(\text{rep.})$ is the cubic anomaly coefficient. The conventions for the second Dynkin index of SU and USp groups are adjusted to be the same as that of SO groups by multiplying an additional factor of 2.

$\text{Tr}(G^3)$ cubic anomaly. Since only gauge groups with matter fields in complex representations can have a cubic gauge anomaly, one only needs to consider $G = SU(N)$. Thus, matter fields in the representation $\oplus_i n_i R_i$ contribute to cubic anomaly as follows

$$\text{Tr}(SU(N)^3) = \sum_i n_i A(R_i), \quad (\text{A.1})$$

where n_i is the multiplicity of the representation of R_i .

$\text{Tr}(U(1)_R G^2)$ anomaly. Contrary to the cubic gauge anomaly, all gauge groups potentially suffer from the mixed anomaly $\text{Tr}(U(1)_R G^2)$. Since both, gauge and matter multiplets contribute, the anomaly can be evaluated via

$$\text{Tr}(U(1)_R G^2) = t_2(\text{adj.}) + \sum_i n_i (r_i - 1) t_2(R_i), \quad (\text{A.2})$$

where the first term is due to the gauginos (R -charge 1), and the second term accounts for chiral superfields of R -charge r_i , transforming in a representation R_i .

$\text{Tr}(U(1)_R)$ and $\text{Tr}(U(1)_R^3)$ anomalies. Lastly, the $\text{Tr}(U(1)_R)$ and $\text{Tr}(U(1)_R^3)$ anomalies can be evaluated via

$$\begin{aligned} \text{Tr}(U(1)_R) &= \sum_\alpha d_{G_\alpha} + \sum_a d_a (r_a - 1), \\ \text{Tr}(U(1)_R^3) &= \sum_\alpha d_{G_\alpha} + \sum_a d_a (r_a - 1)^3, \end{aligned} \quad (\text{A.3})$$

where α and a run over all gauge and chiral matter fields (with R -charge r_a), respectively. The multiplicity $d_a = \dim R_{\text{gauge}} \cdot \dim R_{\text{flavour}}$ of the a -th chiral supermultiplet accounts for the dimensions with respect to the gauge and flavour symmetry representation.

NSVZ β -function. The $\mathcal{N} = 1$ NSVZ β -function of a gauge node is given by

$$\beta\left(\frac{8\pi^2}{g_c^2}\right) \equiv \mu \frac{\partial}{\partial \mu} \frac{8\pi^2}{g_c^2} = \frac{3t_2(\text{adj.}) - \sum_i t_2(R_i)(1 - \gamma_i(g_c))}{1 - \frac{t_2(\text{adj.})}{8\pi^2} g_c^2}, \quad (\text{A.4})$$

where μ is the energy scale, and $\gamma_i(g_c)$'s are the anomalous dimensions of matter fields in representation R_i . Since in this work only the sign of the β -function is relevant, whose denominator is always positive for small enough g_c^2 , one may solely focus on the numerator. Furthermore, the anomalous dimensions are proportional to g_c^2 , which is a second order corrections; thus, for an asymptotically free theory, one requires that the leading order contribution of $\beta\left(\frac{8\pi^2}{g_c^2}\right)$ must be non-negative, i.e.

$$\beta\left(\frac{8\pi^2}{g_c^2}\right)\Big|_{\text{leading order}} \propto \left(3t_2(\text{adj.}) - \sum_i t_2(R_i)\right) \geq 0, \quad (\text{A.5})$$

where $3t_2(\text{adj.})$ originates from the gauge multiplet, and the remainder accounts for the matter multiplets. In fact, the condition (A.5) is sufficient to verify if a theory is asymptotically or IR free, because (A.5) yields the upper bound of the conformal window of the gauge node. For example, consider a $SU(N_c)$ gauge node with N_f quarks $(Q, \tilde{Q})_i$ in the (anti-)fundamental representation, then (A.5) implies that

$$3 \cdot 2N_c - 2N_f \cdot 1 \geq 0 \quad \Leftrightarrow \quad N_f \leq 3N_c, \quad (\text{A.6})$$

which is exactly the upper bound of the conformal window for a $SU(N_c)$ gauge node. Likewise, the statement is valid for $SO(N)$ and $USp(2N)$ gauge nodes too. For instance, consider a $USp(2N_c)$ gauge node with $2N_f$ chiral fields Q_i in the fundamental representation of $USp(2N_c)$ group. Then (A.5) yields

$$3 \cdot (2N_c + 2) - 2N_f \cdot 1 \geq 0 \quad \Leftrightarrow \quad N_f \leq 3(N_c + 1), \quad (\text{A.7})$$

and, again, $3(N_c + 1)$ is precisely the upper bound of the conformal window for a $USp(2N_c)$ gauge group. For a $SO(2N_c)$ gauge group with N_f chiral fields Q_i in the vector representation of $SO(2N_c)$, one can verify that the upper bound is given by $3(N_c - 1)$.

References

- [1] D. Gaiotto and S. S. Razamat, $\mathcal{N} = 1$ theories of class \mathcal{S}_k , *JHEP* **07** (2015) 073 [[1503.05159](#)].
- [2] S. S. Razamat, C. Vafa and G. Zafrir, $4d \mathcal{N} = 1$ from $6d(1, 0)$, *JHEP* **04** (2017) 064 [[1610.09178](#)].
- [3] I. Bah, A. Hanany, K. Maruyoshi, S. S. Razamat, Y. Tachikawa and G. Zafrir, $4d \mathcal{N} = 1$ from $6d \mathcal{N} = (1, 0)$ on a torus with fluxes, *JHEP* **06** (2017) 022 [[1702.04740](#)].
- [4] H.-C. Kim, S. S. Razamat, C. Vafa and G. Zafrir, *E-String Theory on Riemann Surfaces*, *Fortsch. Phys.* **66** (2018) 1700074 [[1709.02496](#)].
- [5] H.-C. Kim, S. S. Razamat, C. Vafa and G. Zafrir, *D-type Conformal Matter and SU/USp Quivers*, *JHEP* **06** (2018) 058 [[1802.00620](#)].
- [6] H.-C. Kim, S. S. Razamat, C. Vafa and G. Zafrir, *Compactifications of ADE conformal matter on a torus*, *JHEP* **09** (2018) 110 [[1806.07620](#)].
- [7] S. S. Razamat and G. Zafrir, *Compactification of 6d minimal SCFTs on Riemann surfaces*, *Phys. Rev.* **D98** (2018) 066006 [[1806.09196](#)].
- [8] J. J. Heckman, D. R. Morrison and C. Vafa, *On the Classification of 6D SCFTs and Generalized ADE Orbifolds*, *JHEP* **05** (2014) 028 [[1312.5746](#)].
- [9] M. Del Zotto, J. J. Heckman, A. Tomasiello and C. Vafa, *6d Conformal Matter*, *JHEP* **02** (2015) 054 [[1407.6359](#)].
- [10] H. Hayashi, S.-S. Kim, K. Lee, M. Taki and F. Yagi, *More on 5d descriptions of 6d SCFTs*, *JHEP* **10** (2016) 126 [[1512.08239](#)].
- [11] M. R. Douglas and G. W. Moore, *D-branes, quivers, and ALE instantons*, [hep-th/9603167](#).
- [12] C. V. Johnson and R. C. Myers, *Aspects of type IIB theory on ALE spaces*, *Phys. Rev.* **D55** (1997) 6382 [[hep-th/9610140](#)].

- [13] A. Hanany and A. Zaffaroni, *Issues on orientifolds: On the brane construction of gauge theories with $SO(2n)$ global symmetry*, *JHEP* **07** (1999) 009 [[hep-th/9903242](#)].
- [14] K. Ohmori, H. Shimizu, Y. Tachikawa and K. Yonekura, *Anomaly polynomial of general 6d SCFTs*, *PTEP* **2014** (2014) 103B07 [[1408.5572](#)].
- [15] K. Intriligator, *6d, $\mathcal{N} = (1, 0)$ Coulomb branch anomaly matching*, *JHEP* **10** (2014) 162 [[1408.6745](#)].
- [16] J. Fuchs and C. Schweigert, *Symmetries, Lie algebras and representations: A graduate course for physicists*. Cambridge University Press, 2003.
- [17] V. Sadov, *Generalized Green-Schwarz mechanism in F theory*, *Phys. Lett.* **B388** (1996) 45 [[hep-th/9606008](#)].
- [18] V. Kumar, D. R. Morrison and W. Taylor, *Global aspects of the space of 6D $N = 1$ supergravities*, *JHEP* **11** (2010) 118 [[1008.1062](#)].
- [19] S. Monnier, *The global anomaly of the self-dual field in general backgrounds*, *Annales Henri Poincare* **17** (2016) 1003 [[1309.6642](#)].
- [20] K. A. Intriligator and B. Wecht, *The Exact superconformal R symmetry maximizes a*, *Nucl. Phys.* **B667** (2003) 183 [[hep-th/0304128](#)].
- [21] D. Gaiotto and H.-C. Kim, *Duality walls and defects in 5d $\mathcal{N} = 1$ theories*, *JHEP* **01** (2017) 019 [[1506.03871](#)].
- [22] C. S. Chan, O. J. Ganor and M. Krogh, *Chiral compactifications of 6-D conformal theories*, *Nucl. Phys.* **B597** (2001) 228 [[hep-th/0002097](#)].
- [23] A. Hanany and A. Zaffaroni, *The master space of supersymmetric gauge theories*, *Adv. High Energy Phys.* **2010** (2010) 427891.
- [24] D. Kutasov, A. Parnachev and D. A. Sahakyan, *Central charges and $U(1)(R)$ symmetries in $N=1$ superYang-Mills*, *JHEP* **11** (2003) 013 [[hep-th/0308071](#)].
- [25] S. Benvenuti and S. Giacomelli, *Supersymmetric gauge theories with decoupled operators and chiral ring stability*, *Phys. Rev. Lett.* **119** (2017) 251601 [[1706.02225](#)].
- [26] N. Yamatsu, *Finite-Dimensional Lie Algebras and Their Representations for Unified Model Building*, [1511.08771](#).